Pathway discovery and eco-physiological relevance of a new enzyme and its products involved in exogenous fatty acid incorporation in cyanobacteria.

Ricardo Júnio Coelho Vitorino de Queirós
Mestrado em Biologia Funcional e Biotecnologia das Plantas
Departamento de Bilogia
2022

Orientadores
Amaranta Kahn, Investigadora Júnior, CIIMAR
Pedro Leão, Investigador Principal, FCUP, CIIMAR

U.PORTO
FACULDADE DE CIÊNCIAS
UNIVERSIDADE DO PORTO

Todas as correções determinadas pelo júri, e só essas, foram efetuadas.

O Presidente do Júri,

Declaração de Honra

Eu, Ricardo Júnio Coelho Vitorino de Queirós, inscrito(a) no Mestrado em Biologia Funcional e Biotecnologia das Plantas da Faculdade de Ciências da Universidade do Porto declaro, nos termos do disposto na alínea a) do artigo 14.º do Código Ético de Conduta Académica da U.Porto, que o conteúdo da presente dissertação/relatório de estágio/projeto [indicar o aplicável] reflete as perspetivas, o trabalho de investigação e as minhas interpretações no momento da sua entrega.

Ao entregar esta dissertação/relatório de estágio/projeto “Pathway discovery and eco-physiological relevance of a new enzyme and its products involved in exogenous fatty acid incorporation in cyanobacteria”, declaro, ainda, que a mesma é resultado do meu próprio trabalho de investigação e contém contributos que não foram utilizados previamente noutros trabalhos apresentados a esta ou outra instituição.

Mais declaro que todas as referências a outros autores respeitam escrupulosamente as regras da atribuição, encontrando-se devidamente citadas no corpo do texto e identificadas na secção de referências bibliográficas. Não são divulgados na presente dissertação/relatório de estágio/projeto “Pathway discovery and eco-physiological relevance of a new enzyme and its products involved in exogenous fatty acid incorporation in cyanobacteria” quaisquer conteúdos cuja reprodução esteja vedada por direitos de autor.

Tenho consciência de que a prática de plágio e auto-plágio constitui um ilícito académico.

Ricardo Queirós

Porto, 26 de outubro de 2022

Acknowledgements

I would like to start by thanking Pedro Leão for allowing me to develop my master thesis in the CNP Lab. Not only is he an amazing scientist and teacher but has also built an incredible team for his lab. It has indeed been a great time spent with this team that not only has developed great science but also a great work environment that could make the laziest and most uninspired person into another great team member if needed. I want to thank all of the lab members for your support and motivation. A special thanks is owed to my mentor and friend Amaranta Kahn, I could not have the luck to get such a great person as my mentor for my thesis, so I want to thank her for allowing me to develop her (and now mine) work in the most enjoyable way possible. Thank you all for the scientific and social experiences you have given me even when I wasn't the most sociable person! So, thank you Bárbara and Diana for having the concern to inform me of important events and information throughout the year! Sara, Raquel, Ana, Eunice, Anne, Teresa, Adriana, Lígia and Kat for always being available to help me with my doubts and problems. The same for the guys of the lab, thank you João for your expertise and humor throughout the year, Paulo and Marco for your amazing knowledge and help at every turn. I sincerely look up to all of you in a lot of aspects as role models to follow in my future! A special thanks to Axel and Aldo for their help in developing the statistical part of my thesis and for being available so often for my work.

This work was supported by national funds through FCT – Fundação para a Ciência e Tecnologia, I.P. under the framework of the project with reference "PTDC/BIA-BQM/5760/2020" and through grants UIDB/04423/2020 and UIDP/04423/2020. This work was developed under the European Research Council through a Starting Grant (759840) and the European Union's Horizon 2020 programme (WIDESPREAD, Grant Agreement 952374).

Abstract

Fatty acids (FAs) are a group of important molecules, used in industry, bioenergetics and for life in general. They are key metabolite in microorganisms, playing critical roles in carbon and energy storage, as well as in synthesis of complex lipids and secondary metabolites. Cyanobacteria are a known group of gram-negative bacteria that produce an unusual high number of secondary metabolites derived from FAs. Recently, a new cyanobacterial enzyme responsible for producing such metabolites, the BrtB enzyme, has been reported. BrtB was found to directly (without former activation) esterify free exogenous fatty acids (eFAs) with a family of abundant glycolipids, the bartolosides, resulting in bartoloside fatty acids (B-FAs). As eFAs microbial incorporation is known to happen only via activation of the FAs (through the Acyl-acyl carrier synthetase (Aas)), we regarded the BrtB pathway as a new putative pathway of eFAs incorporation. Therefore, we set out to investigate the eco-physiological role of bartolosides and B-FAs in the cyanobacteria of their discovery *Synechocystis salina* LEGE 06099 (*S. salina* 06099). With this goal in mind, we first attempted to knock-out BrtB and the Aas genetically and/or chemically from *Synechocystis salina* LEGE 06099. We then studied the growth of *S. salina* 06099 as well as its bartolosides and B-FAs content under various environmental conditions (temperature, light and CO_2) and over time. We found that B-FAs level was highly increased upon supplementation with eFAs, increased under lower temperature (17°C in contrast to 23/30°C), slightly decreased under light or CO_2 stress conditions, and that their composition in unsaturated FAs was higher at a higher temperature, as well as under light and CO_2 stress conditions. Lastly, we cloned and performed a heterologous expression of two lipases that could be regarded as hydrolyzing the esters of the B-FAs. These will be expressed in a larger scale for future characterization.

Resumo

Os ácidos gordos (FAs) são um grupo de moléculas importantes, seja na indústria, na bioenergética e para a vida em geral. São metabolitos fundamentais em microrganismos, desempenhando papéis críticos no armazenamento de carbono e energia, bem como na síntese de lípidos complexos e metabolitos secundários. Cianobactérias são um grupo conhecido de bactérias gram-negativas que produzem um número incomum de metabolitos secundários derivados de FAs. Recentemente, foi reportada uma nova enzima cianobacteriana responsável pela produção de tais metabolitos, a enzima BrtB. A BrtB foi encontrada diretamente (sem a ativação anterior) a esterificar ácidos gordos exógenos livres (eFAs) com uma família de glicolipídeos abundantes, as bartolosidas, resultando em ácidos gordos bartolosida (B-FAs). Como a incorporação microbiana dos eFAs só acontece através da ativação dos FAs (através da "Acyl-acyl carrier synthetase" (Aas)), consideramos a via BrtB como uma nova via putativa de incorporação de eFAs. Assim, partimos para investigar o papel eco-fisiológico das bartolosidas e B-FAs nas cianobactérias onde foram descobertas, a *Synechocystis salina* LEGE 06099 (*S. salina* 06099). Com este objetivo em mente, tentámos pela primeira vez fazer knock-out do BrtB e da Aas geneticamente e/ou quimicamente na *Synechocystis salina* LEGE 06099. Estudamos então o crescimento da *S. salina* 06099, bem como os seus bartolosides e conteúdo de B-FAs em diversas condições ambientais (temperatura, luz e CO_2) e ao longo do tempo. Constatámos que o nível B-FAs foi altamente aumentado após a suplementação com eFAs, aumentou a uma temperatura mais baixa (17°C em contraste com 23/30°C), diminuiu ligeiramente em condições de stress luminoso ou depleção de CO_2, e que a sua composição em FAs insaturados era mais elevada a uma temperatura mais elevada, bem como em condições de stress luminoso e depleção de CO_2. Por último, clonámos e executámos uma expressão heteróloga de duas lipases que poderiam ser consideradas como hidrolises de ésteres dos B-FAs. Estas serão expressas numa escala maior para a caracterização futura.

Keywords

Secondary metabolites; Cyanobacteria; Bartolosides; Exogenous Fatty Acids; *Synechocystis salina* LEGE 06099; Bartolosides ester; Acyl-acyl carrier synthetase.

List of Abbreviations

Aas	Acyl-acyl carrier protein synthetases
ACP	Acyl carrier protein
AMS-C10	[5′-O-(N-decanylsulfamoyl)Adenosine])
AUC	Area under the curve, obtained through Xcalibur program using LC-MS data
AUC/C	Area under the curve normalized per cell
B-FA	Bartoloside fatty acid
eFA	Exogenous fatty acid
FA	Fatty acid
FAS	Fatty acid synthase
FFA	Free fatty acid
HRESIMS	High resolution electron spray ionization mass spectrometry
IPTG	Isopropyl β-D-1-thiogalactopyranoside
Kan	Kanamycin
KO	knock-out
LC-MS	Liquid chromatography-mass spectrometry
Lip A	Lipase A
Lip 0482	Lipase 0482
MeOH	Methanol
O.D.	Optical density
OE	Organic extraction
ON	Over-night
PCC	Pasteur culture collection
PCC 6803	*Synechocystis sp.* PCC 6803
rpm	Revolutions per minute
WT	Wild type
06099	*Synechocystis Salina* LEGE 06099
6803 *Aas*	*Synechocystis sp.* PCC 6803 with a knock-out on the Aas gene

Table of Contents

List of Figures and Tables

1 - Introduction

1.1 - Fatty acids: cellular key metabolites

Fatty acids (FAs) are important molecules in bioenergetics and in industry. They are mostly insoluble in water and organize spontaneously to form micelles. They are essential and central key metabolites representing an important source of metabolic energy to all organisms (Currie et al.,2020).

All-size FAs are known for decades to covalently bind to hundreds of different proteins, resulting in fatty acylating proteins. The acylation of those proteins confers them separate biochemical properties related to regulation of intracellular trafficking and signaling, subcellular localization, protein-protein, protein-lipid interactions and targeting (Resh 1999, Resh 2016).

FAs also play an important role in carbon and energy storage in the form of neutral lipids or lipid droplets (Wältermann and Steinbüchel 2005). Nevertheless, most FAs are utilized for the synthesis of complex lipids as essential components of cell membranes. Additionally, FAs can be found in many secondary metabolites. As such, in cyanobacteria, as in every organism, *de novo* production of FAs is critical to the cell. This explains why, many antibiotics are directed towards bacterial FAs synthesis pathway, leading to the microorganism death (Currie et al., 2020).

1.2 -Cyanobacteria and their particular fatty acid metabolism

One group of gram-negative prokaryotes, Cyanobacteria, are specifically known to possess an unusually high amount of those derived FAs secondary metabolites, as well as to have a singular FA metabolism. Indeed, the β-oxidation pathway, which is the FAs degradation pathway characterized in both eukaryotes and prokaryote, is an important catabolic process that uses fatty acids as energy and carbon sources. β-oxidation shortens the saturated acyl-CoA by two carbons in each step to finally produce acetyl-CoA (Azim and Shoukat, 2009). However, this mechanism was not yet was not found to be present in cyanobacteria. This might explain such a high quantity of FAs secondary derived metabolites present in this group (Figueiredo et al., 2021). Cyanobacteria are mainly aerobic photoautotrophic, and so sustain themselves only through water, carbon dioxide, inorganic substances, and light (Huisman et al. 2018). Their metabolism and biomolecule generation are mainly achieved by fixing carbon dioxide as they do not need other substrates to be available (Sanchez-Beracaldo et al., 2022). If *de novo* production

of FAs is critical to organisms, it remains a costly process both in terms of energy and material deployed by the cell. To mitigate that cost, microorganism, including

cyanobacteria, evolved pathways allowing the incorporation of exogenous fatty acids (eFAs) directly from their environment (Yao and Rock, 2017).

Cyanobacteria diversity, morphology, metabolism, and genetics allowed them to colonize many ecosystems, ranging from terrestrial to aquatic environments (freshwater and saltwater) (Budel et al., 2011). After such a long evolutionary history, they possess today very diverse lifestyle as well as being morphologically and metabolically different (Ford et al. 2021). These organisms, which constitutes a large part of the phytoplankton, have an essential role in the nitrogen and carbon cycle (Zhang et al., 2018). However, FA metabolism seemed mostly conserved among cyanobacteria. Endogenous synthesis of new FAs and further esterification into lipids most commonly occurs using a collection of enzymes organized as fatty acid synthase II (FAS II) pathway. While a lot is known about the essential role of endogenous FAS II, activation, initiation, elongation, and transfer to the membrane bilayer (Currie et al., 2020), eFAs transfer across biological membranes and other enzymes involved in their uptake still remains poorly characterized (von Berlepsch et al., 2012). Two proteins involved in the transportation out of Synechocystis sp. PCC 6803 were reported, along with one other cyanobacteria that used flip-flop method of diffusion for free fatty acid across the membrane (Bellefleur, et al., 2019). eFAs incorporation pathway in cyanobacteria, however, was previously reported to necessarily involve the activation of the eFAs coupled to its incorporation, into to the thiol of acyl carrier protein (ACP), a co-factor in FA biosynthesis. To be

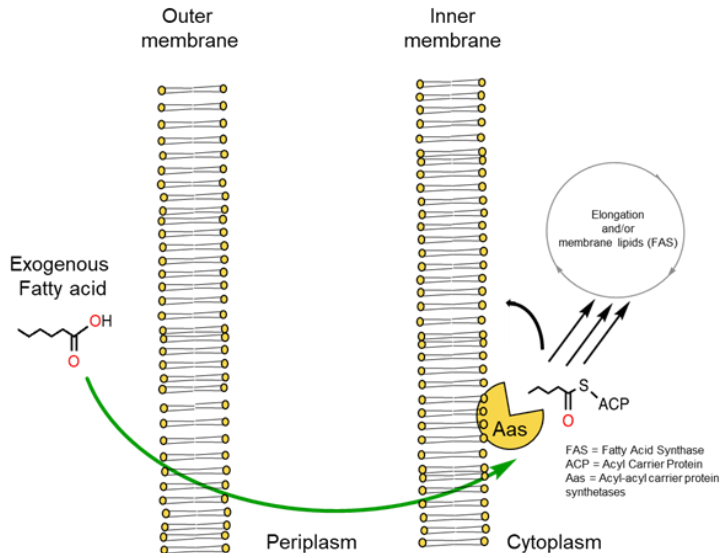

Figure 1 - Scheme of the Exogenous fatty acid (eFA) incorporation pathways present in cyanobacteria. Aas cellular localization has not yet been elucidated for all cyanobacteria, but it has been reported to be attached to the membrane in PCC 6803.

activated and incorporated into lipids, eFAs must be prior loaded onto the active form of ACP to give an acyl-ACP. They could thus enter lipid biosynthesis pathways or enter further FA endogenous metabolism through the FAS II pathway.

The enzyme that has been identified as responsible for the incorporation coupled to the activation of eFA stands by the name acyl-acyl carrier protein synthetases (Aas) (Kaczmarzyk and Fulda, 2010). It was first identified in the model strain cyanobacterium *Synechocystis* sp. PCC 6803 (PCC 6803) and was reported to be the key enzyme for the promiscuous incorporation and activation of eFAs in this organism (Kaczmarzyk and Fulda, 2010) (Figure 1). It was further shown to be conserved in cyanobacteria. By that mean, eFAs incorporation would provide an alternative and cheaper way than the endogenous FAS II pathway to provide FAs to the cell. Furthermore, this would also allow microorganisms a possible adaptation of the lipid composition to environmental condition changes, such as high-stress or nutrient limiting conditions (Kaczmarzyk and Fulda, 2010).

1.3 - Bartolosides, bartolosides fatty acids and BrtB

As the Aas was thought to be the only enzyme responsible for eFAs incorporation in cyanobacteria, the Leão lab recently reported a new enzyme esterifying eFAs, that could act prior to eFA activation (Reis et al., 2020) (Figure 2). This cyanobacterial enzyme - BrtB- was found to be responsible for direct esterification between free fatty acids (FFAs) and alkyl halide moieties of a family of abundant glycolipids, the bartolosides, into resulting bartoloside fatty acid esters (B-FAs), whose biosynthesis is encoded by the brt gene cluster. Bartolosides and the brt gene cluster were first discovered in several marine non-model cyanobacterial strains, such as Synechocystis salina LEGE 06099 (S. salina), where it can be as abundant as 1% of bacterial dry weight, while not showing relevant cytotoxic or antimicrobial activities (Afonso et al., 2016, Leao et al., 2015). All bartolosides are chlorinated dialkylresorcinol and can be divided into two groups according to their structure: i) monoglycosylated versions, containing an O-linked β-D-xylosyl moiety and ii) diglycosylated versions featuring an O-linked α-L-rhamnose and a C-linked xylose while additional differences consist in the alkyl chain length that can range from 11 to 15. B-FAs are created by the attack of the fatty acyl carboxylate onto the chlorinated carbon in the bartolosides, removing the chlorine atom (Reis et al. 2020). Bartoloside A and its B-FAs were found to be most abundant in the strain Synechocystis Salina LEGE 06099 (S. salina 06099). After supplementing S. salina 06099 with exogenous FAs (eFAs), Reis and colleagues observed a drastic cellular reduction of bartoloside (>99%) concomitant with the raise of the same amount of its esterified

counterpart, the B-FAs. Additionally, they showed that BrtB: 1) does not need free FAs (FFAs) to be activated by the Aas for it to be esterified with bartolosides, 2) does not seem to accept acids other than FAs, 3) can accept a wide range of FAs (C2 to C18) aswell as unsaturated versions. Therefore, this enzyme generates a diversity of B-FAs, and its promiscuity is compatible with a new system intended to capture eFAs, that could then be further elongated and/or utilized. However, the regulation of this system, the associated cellular locations, the function, the eco-physiological relevance of its products and the recycling of the pathway remain unknown.

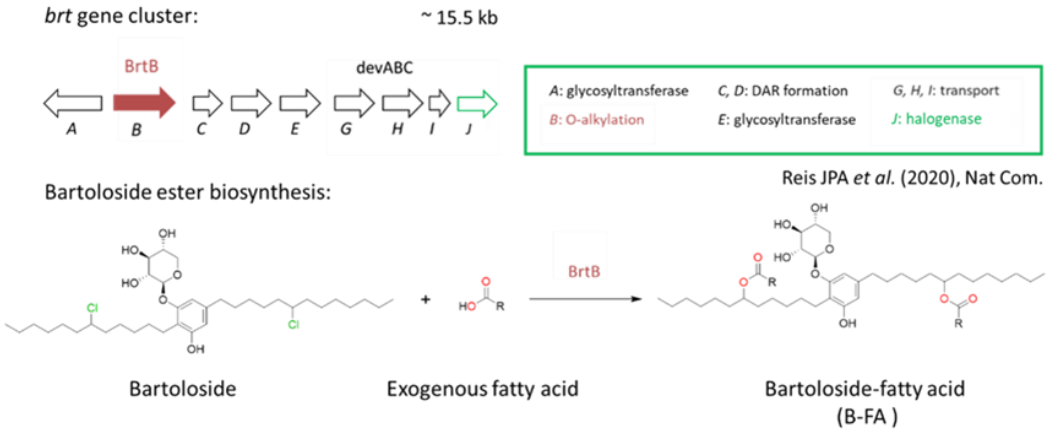

Figure 2 - Representation of the composition of the brt gene cluster, and of the bartoloside ester biosynthesis by the BrtB enzyme. The BrtB enzyme can esterify bartolosides with a fatty acid by replacing the chlorines present in the compound with the fatty acid to form a new natural product named Bartoloside Fatty acid (B-FA).

1.4 - The hypothesis

We hypothesized that B-FAs could represent a new eFA incorporation mechanism (Figure 3), in the view of further incorporation and possible storage of eFAs in the cell, eventually less costly than the endogenous system already present in cyanobacteria and allowing the microorganism to make use of available FFAs of its surrounding.

This mechanism would differ from the Aas one, as it would uptake and further incorporate

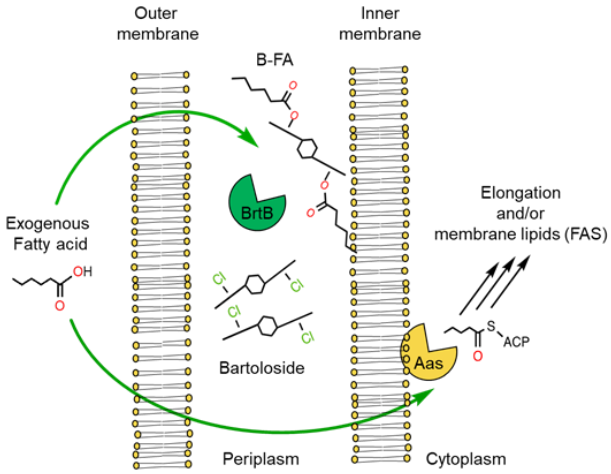

Figure 3 – Proposed exogenous fatty acid (eFA) incorporation pathway hypothesis, based on the discovery of bartolosides, B-FAs and its enzyme BrtB. The localization of all the pathway effectors is not yet determined however, BrtB is predicted to be membrane bound and was found to act prior/instead of the Aas in labelled FAs supplementation experiments.

eFAs into the cell without activating the eFAs. Previous data in the lab already confirmed that eFAs could indeed be picked up by BrtB prior to the Aas (no activation was found upon incorporation), and further incorporated into B-FAs. The present project is focused on the understanding of the pathway, the function and eco-physiological relevance of this new *brt* system and its effector, as well as its recycling.

The first priority was the creation of a genetical and chemical knock-outs of the *brt* and *aas* gene, in order to study the *brt* system pathway. Second, the relevance (level) of those bartoloside and B-FA over time, and under different feeding and environmental conditions (temperature, light, CO_2) was evaluated. Followed by the study of the recycling of those FAs incorporated in B-FA by heterologous expression of two lipases in *Escherichia coli* (*E. coli*), which could be responsible for the FAs hydrolysis of the B-FAs.

2 - Results and Discussion

2.1 - Aas and BrtB KOs in S. salina 06099

2.1.1 - Genetic KO: Natural transformation

A straightforward way to characterize the BrtB pathway, the function of its effectors, to compare it to the Aas pathway, and to assess the eventual fitness it confers to its host, would be to KO the BrtB and Aas enzymes from *S. salina* 06099. This would allow the carrying of various growth experiments under different conditions to be compared to the wild type (WT). Thus, the generation of two single mutants lacking *aas* and the *brtB* genes in *S. salina* 06099.

To do so, the utilization of natural transformation (NT) was envisioned, as it was previously described many times to be successful in PCC 6803 (Kufryk et al.,2002, Pope et al., 2020). Indeed, PCC 6803 is a very genetically close organism of *S. salina* 06099, and all the pili machinery required for NT (Chen et al., 2020) is found in 06099 (previous observation). According to previously described successful NT, the pBlueScript II SK(+) vector (Figure 4) was used with either an Aas KO insert (2589 bp) or a BrtB KO insert

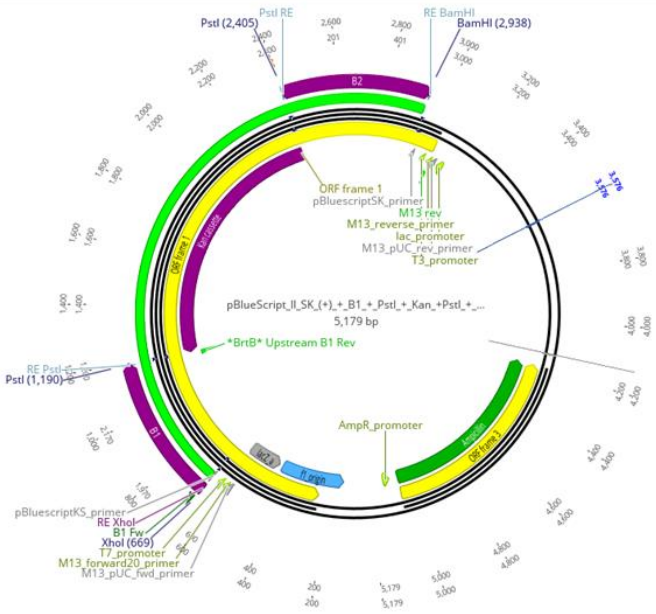

Figure 4 - Example of the pBlueScript II SK (+) vector used that carries the construct of interest (flanking regions of BrtB gene up and downstream of a kanamycin resistance cassette) between XhoI (669) and BamHI (2938) restriction enzymes sites, f1 origin (f1), T7 promoter, T3 promoter, ampicillin resistance ORF, pUC replication origin (ori), LacZ_a (β-galactosidase α-fragment) coding sequence and lac promoter.

(2269 bp). Both inserts consisted of two flanking regions of the respective gene with a kanamycin resistance cassette (1215 bp) in the middle, as well as designed their respective primers. Utilizing the constructs, two complementary fragments of the

upstream and downstream part of either the Aas or the BrtB gene would be incorporated in the genome through homologous recombination, along with, in between those two fragments, a kanamycin resistance cassette replacing the gene of interest.

It has been shown that DNA introduced into *Synechocystis* PCC 6803 (PCC 6803) may replicate independently from a suitable plasmid or be inserted into the genome via double homologous recombination (Pope et al., 2020). Various trials of NT were performed on *S. salina* 06099 (06099), but none were successful. In cyanobacteria full segregation of KO through the entire genome is not straight forward, as cyanobacteria possess multiple genomes copies per cell (from 12 to 142 copies were reported). This makes it difficult to fully segregate the mutation, requiring multiple streaking of single colonies in antibiotic growth cultures (Pope et al., 2020).

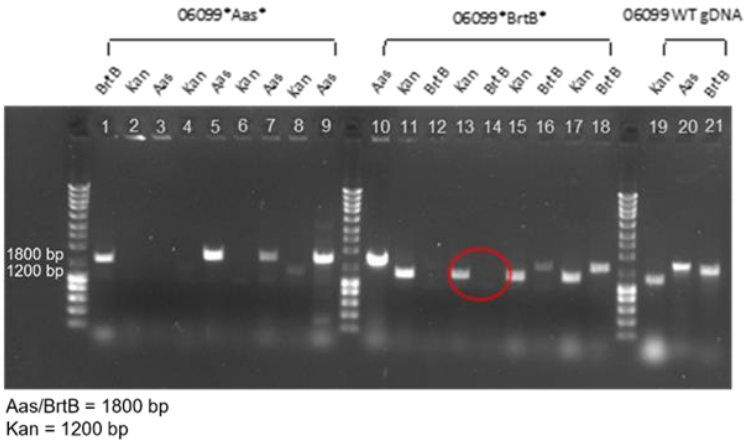

Figure 5 - Colony PCR performed on *S. salina* 06099 colonies grown in kanamycin antibiotic plates, to determine its segregation status upon natural transformation assay. NZYDNA Ladder III (200 bp to 10000 bp) was used as a marker. Successful KOs, fully segregated will show a lack of band at 1800 bp (Aas/BrtB gene) and the presence of a band at 1200 bp (Kanamycin resistance cassette (Kan)). Positions 1, 10, 19-21 are control bands. After control bands, single colonies are grouped in pairs (2-3,4-5, etc…). Example of possible successful KO in position 13 and 14, which show presence of kanamycin cassette and lack of BrtB gene. All colonies used in this colony PCR were replated in same or higher kanamycin concentration BG 11 plates.

After each NT transformation, to test the segregation of the transformed genome, colony PCRs were performed on colonies grown in Kan antibiotic plates (Figure 5). Their survival on Kan antibiotic plates ensured the plasmid incorporation by acquiring the antibiotic resistance, however, it cannot prove a full segregation. A successful colony PCR would show a band for the Kan cassette and not show a band for the gene to be knocked out, while the presence of both would mean replating the colony on a higher antibiotic concentration, applying more selective pressure on the colony, in theory, forcing it to segregate the KO across its genome to survive. We can see in the 7th and 8th positions (Figure 5) one mutant that is not fully segregated, possessing both the Kan resistance cassette and the *aas* genes which should have been entirely removed if the

segregation was total. We can also observe in the second part of the gel, correspondent to the *brtB* KO, that all tested colonies possess the Kan cassette, but all except the middle wells (14th and 15th wells), still show *brtB* presence in the genome (the middle colonies were replated, but later proved unsuccessful to segregate).

As it was said, full segregation upon NT were unsuccessful after multiple attempts. Currently, the strain capacity of acquired external DNA is being tested by the mean of other techniques available. First, we took a small step back by testing the incorporation of a small plasmid with no insert, to test whether the cell could accept foreign DNA. Next other techniques will also be tested, mainly, electroporation and conjugation, to genetically engineer *S. salina* 06099.

2.1.2 - Chemical KO of the Aas: the AMS C-10

As an alternative solution, since any fully segregated KO has yet to be obtained successfully, we envisioned, for the *aas* gene, the possibility of using a chemical inhibitor. A recent chemical inhibitor of the Aas have been developed by Curie et al. in *Vibrio harveyi,* and *Vibrio cholerae*, both gram-negative bacteria. The inhibitor AMS-C10 [5′-O-(Ndecanylsulfamoyl)adenosine] mimics the tightly bound acyl-AMP reaction intermediate and was reported to prevent further activation of the Aas pathway in both *V. harveyi* and *V. cholerae*, stopping eFA incorporation via the Aas system. Prior to the start of thesis, the Aas gene from the strain *S. salina* 06099 had already been expressed heterologously in *E. coli* and further purified. The AMS-C10 inhibitor was then *tested in vitro* and shown to inhibit the formation of acyl-ACP upon its addition the purified Aas, ACP and FAs. To test its *in vivo* efficiency and to calibrate/optimize it, small scale experiments were first conducted, followed by a larger scale experiment from which the *S. salina* 06099 lipids could be extracted. As a start, it was tested, in 96 wells plates, various concentrations of the AMS-C10 with the cyanobacterial strains to test its toxicity, as well as the toxicity of different mix of FAs. Additionally different concentrations of cerulenin, a compound inhibiting the FAS II pathway (Currie et al., 2020) and leading to cell death, were tested to investigate whether feeding of eFAs could rescue cyanobacterial growth using the Aas, or just using BrtB. To start with the template from the previously described experiments of Currie et al., was used, which consisted of the following: i) Cerulenin, ii) AMS-C10, iii) FA mix concentrations to test cell recovery and AMS-C10 toxicity and effectiveness. We tested those different conditions on i) *S. salina* 06099, ii) PCC 6803 model strain (that do not possess the *brt* pathway), and iii) a PCC 6803 *Aas* KO (previously engineered in the lab) as a control.

Table 1 - Different conditions to evaluate the AMS-C10 cytotoxicity, and efficiency in cyanobacteria, as well as to evaluate the Aas pathway and its relationship with the FASII. The tests were performed in triplicates, in three different strains: 1) *S. salina* 06099, 2) PCC 6803, 3) 6803 *Aas*. A and A2 refer to controls of each strain. *DMSO was added to second control accounting to the solvent used for cerulenin and AMS-C10.

A	A2	B	C	D	E
Strain	Strain (FA mix + DMSO*)	Strain + X AMS-C10	Strain + X cerulenin	Strain + FA mix + cerulenin	Strain + FA mix + cerulenin + AMS-C10

Currie et al. (2020) reported no toxicity of the AMS-C10 up to 50 µM concentration on *V. harveyi,* and *V. cholerae* cultures. Additionally, they showed that, the cerulenin inhibition of the previously studied bacteria FASII pathway led to cell death, but that supplementation of eFAs to the culture led to the recovery of the culture, due to eFA incorporation by the Aas.

They proved that the Aas was responsible for the eFAs incorporation by adding AMS-C10 to the cerulenin mix, which led to cell death despite eFA supplementation.

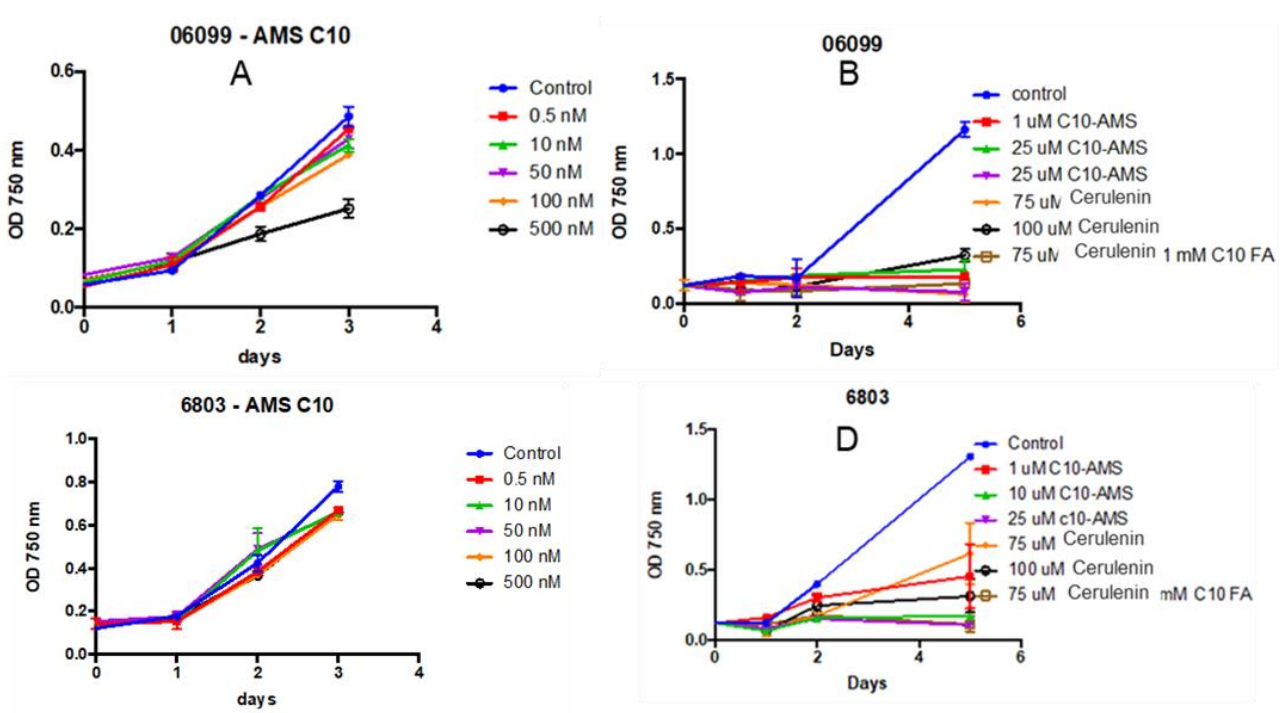

Figure 6 - Graphical data representing AMS-C10 and cerulenin assays, following 96 wells plate optimization assays based on Currie et al., 2020. Various concentrations of AMS-C10 and cerulenin were tested, along with a cell recovery test. Graph A describes optimal concentration tests using AMS-C10 with *S. salina* 06099; Graph B describes initial AMS-C10 tests in *S. salina* 06099 following assays performed on Currie et al., 2020; Graph C and D describe the same but for the model strain PCC 6803. Each condition was performed in triplicate, the data represent the mean ± standard deviation.

The concentrations found specifically for the cyanobacterial strains differed substantially from Currie et al. (2020), which had 50 µM of AMS-C10 to be the optimal concentration, while in cyanobacterial assays 0.1 uM was the more adequate concentration (figure 6 - A) to be the more adequate concentration. And while Currie et al. (2020) established 5 µM of cerulenin as optimal for on *V. harveyi,* and *V. cholerae*, the assays performed showed that 100 µM of cerulenin caused cell death in the cyanobacteria tested (figure 6). In terms of FA mix concentration, after testing, we ended up using the same 1 mM concentration of FAs as a higher concentration could be toxic for the cells. We could not progress further with the cerulenin assay, as the cerulenin plus FA was not allowing cell recovery as described by Currie et al. (Figure 6), for a reason that we cannot yet explain.

Afterwards, a larger scale experiment was conducted to be able to run the resulting samples through LC-MS, where a PCC 6803 culture was pulse fed, with both deuterated (stable isotope) labelled FAs and AMS-C10. Using LC-MS afterwards would allow to check for labelled FA incorporation into lipids: if the AMS-C10 inhibition would be successful, none (or few) of the labelled FA would be found in lipids. A previously performed supplementation experiment with PCC 6803 *Aas*, without the AMS-C10, served as a control. It was observed indeed that the genetic KO of the Aas prevented the incorporation of labelled FAs in 6803 lipids (Annex Figure 1).

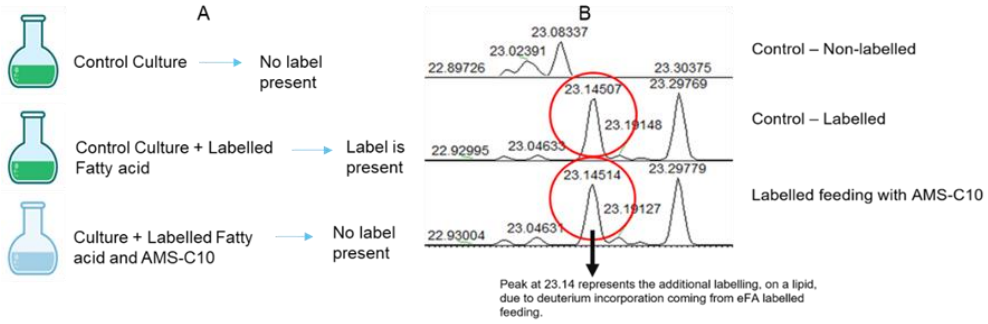

Figure 7 – AMS-C10 assay in larger culture scale. A presents the expected results of a successful AMS-C10 incorporation. B represents the results of AMS-C10 feeding with labelled FA. FA show the same incorporation with and without AMS-C10 in presence of labelled FA.

The organic extraction on the supplemented culture was then analyzed by LC-MS. We observed labelled lipids in both control (no AMS-C10) and AMS-C10 supplemented culture, indicating that the AMS-C10 was not successful in stopping FA incorporation (Figure 7). Different concentration tests all led to the same results. More optimization tests could be realized by changing various conditions that might be stopping *in vivo* success, such as pH conditions, culture media composition, culture concentration, and others, as the AMS-C10 stability in the described conditions might not have been reached. However, further testing of the AMS-C10 as a chemical inhibitor of the Aas pathway in 06099 as yet to be completed.

2.2 - Study of bartoloside and B-FA baseline production in S. salina 06099

With the intent to understand the eco-physiological role of bartoloside and B-FAs in *S. salina* 06099 the production levels across time and under various temperatures was investigated. Indeed, membrane lipids and their FAs compositions were previously shown to be remodeled in a temperature-dependent way, to provide the organism stronger adaptation to temperature changes (Gombos et al., 1992, Murata, 1989, Nalley et al., 2018, Raven-Geider, 1988).

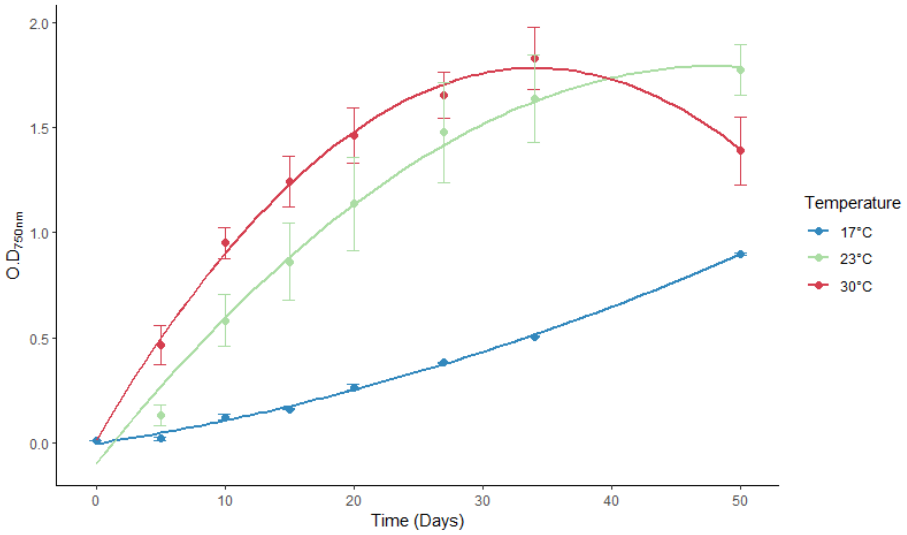

Figure 8 - Growth curve depicting the differences between 17, 23 and 30°C on the growth of the cyanobacteria *S. salina* 06099 based on O.D. over time (50 days). Growth experiments were performed in triplicate, the data represent the mean ± standard deviation.

The investigation followed bartoloside A and B-FA A production in *S. salina* LEGE 06099 as it has been reported to possess the highest amount of bartoloside A (Afonso et al., 2016). From now on, bartoloside or B-FA will refer to bartoloside A or the sum of both mono and bi esters B-FA As, respectively.

S. salina 06099 was grown at three different temperatures to determine its optimal growth conditions.

S. salina 06099 growth lasted 50 days, as cyanobacteria grows slower than well-studied laboratory bacteria. The growth was conducted under a standard light cycle of 16/8h light/dark cycle at 55 µmol m^{-2} s^{-1} light intensity and shaking at 100 rpm. In addition, investigating the presence of B-FA without additional external source of eFA, would determine whether the *brt* system would be active and have a role without supplementation as well. During the growth experiment, samples were collected periodically, and their OD was measured to draw a growth curve (figure 8). The

temperature of 30°C was found to be the optimal growth conditions, similarly to 23°C , observing that both grew much faster than at 17°C.

Simultaneously, the same time points were sampled for organic extraction (OE). After conducting LC-MS analysis and data analysis normalized by cell, the production of bartoloside and their B-FAs was compared and ordered by temperature over 50 days (Figure 9). No data are reported at day 5 and 10 at 17°C as the biomass was not sufficient for OE. No data is reported at day 50 at 30°C as all the cells were dead by this time.

The effect of temperature over time was analyzed with an Analysis of Variance (ANOVA)

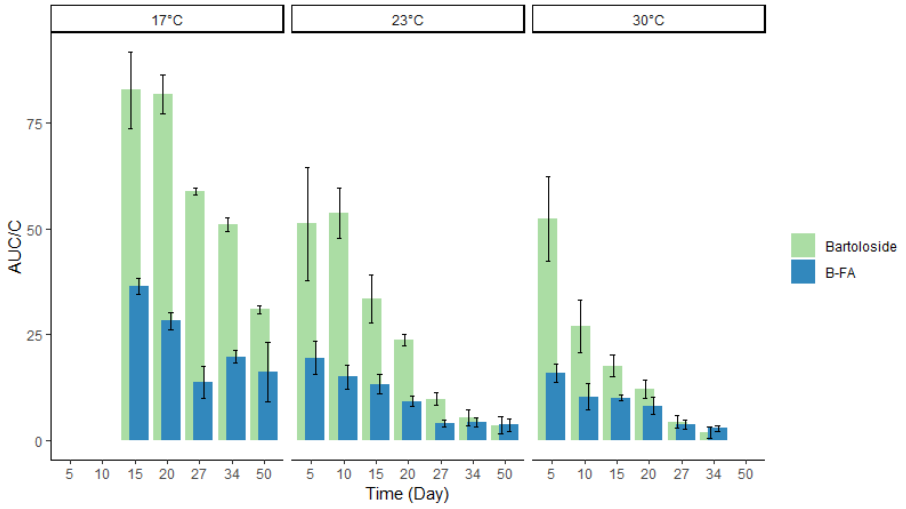

Figure 9 - Evolution of bartoloside A and B-FAs over time and temperature in *S. salina* 06099. Growth experiments were performed in triplicate (except for 17°C, which was done in duplicate), the data represent the mean ± standard deviation (SD). The LC-MS analysis was performed on Xcalibur where respective area under the curve (AUC) was extracted for each mass. AUC was then normalized in AUC per cell (AUC/C).

using temperature as categorical factor and time (log transformed to achieve linear relationship) as numeric covariate. The assumption of normality (Shapiro-Wilks test; p = 0.08 for bartoloside, p = 0.09723 for B-FA) was met for bartolosides and B-FA and the homogeneity of variances (Levene test; p = 0.37 for bartolosides) was only met for bartolosides, so in this case, assumption of variance homogeneity of B-FA for the groups of temperature were weighed by the inverse of their standard deviation. The effect of time was significant and negative (meaning a decrease of bartoloside and B-FA was observed) (Annex, Table 1 and 4). The effect of temperature was also significant (Annex, Table 2 and 5). And there were significant differences found between all pairwise comparisons of temperature levels (Annex, Table 3 and 6). We observe a higher amount of bartoloside and B-FA per cell at the lowest temperature, and at the early stages of culture growth. It is also observed that a higher amount of bartoloside translates into the same concomitant rise in B-FA. The decrease in B-FA concentration at later stages of growth might be connected to the lowering of bartoloside production. If we cannot conclude a role of the bartoloside and B-FAs from this early-stage analyses, we can still

observe that – just like – membrane lipids, bartolosides and B-FAs are affected by temperature growth.

It was reported that, under lower temperature conditions (10°C), PCC 6803 cellular membrane was found to have been composed of more unsaturated FAs, which granted tolerance to low temperatures (Gombos et al., 1992). In another cyanobacteria, *Anabaena variabilis*, the same results were observed. Additionally, the effects of higher temperatures were also tested (38°C) and the increase of saturated membrane FA was observed (Murata and Sato, 1980, Murata, 1989). So, it was generally stated that, on one side, at higher temperatures, cyanobacteria had their membranes enriched in more saturated FAs lipids, which lead to an increase in rigidity, on the other side, at lower temperatures, the membrane is instead composed of unsaturated FA which leads to

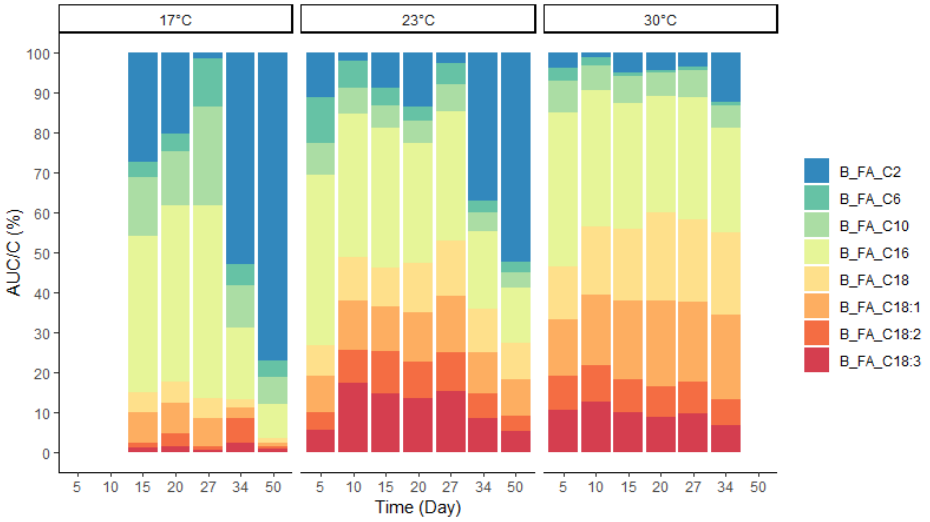

Figure 10 - Proportion of B-FAs A in *S. salina* 06099 over time and temperatures. Growth experiments were performed in triplicate). The LC-MS analysis were performed on Xcalibur where respective area under the curve (AUC) was extracted for each mass. AUC was then normalized in AUC per cell (AUC/C).

enhanced membrane fluidity (Murata and Sato, 1980, Murata, 1989, Nalley et al., 2018). Analyzing B-FA production in more detail, we sought to obtain B-FA diversity of FAs. Firstly, as expected it was observed that B-FAs are promiscuous to FA length (Figure 10).

The diversity of B-FA produced at different temperatures shows a much higher percentage of longer chain FA produced at higher temperatures. We could have expected that B-FA would follow the same trend as lipid FAs, meaning that more unsaturated B-FAs were expected at lower temperature. However, the percentage of unsaturated B-FA increased at higher temperatures. As unsaturated FA lipids are reported to provide a higher membrane flexibility required to adapt to lower temperatures in PCC 6803 (Gombos et al., 1992), *A. variabilis* (Murata, 1989) its expectable for B-FA to not be located directly in the membrane, acting more as a reservoir of recycled FAs, or to have a different role other than membrane fluidity.

On the other hand, B-FA C16 is consistently the most produced over any of the temperatures. Palmitic Acid (C16 FA) has been shown to be the most abundant in intracellular lipids and FFA in cyanobacteria including *Synechocystis* strains, in high content, sometimes reaching >50%, increased by higher temperatures (Eungrasamee et al., 2020, Nalley et al., 2018). This could imply that B-FAs are formed in a non-specific manner by esterification of the available pool of FAs in the cell.

2.3 - Additional environmental conditions variations and their effect on B-FA production

Based on the results described above additional carbon sources and environmental conditions that were reported to affect membrane FA composition (Sakamoto and Bryant, 2002, Takatani et al., 2015, Wang et al.,2020, Cuellar-Bermudez et al., 2015) were investigated, such as light cycle (continuous light versus 16/8h light/dark cycle) and CO_2 abundance. And taking into account the primary hypothesis that this mechanism is responsible for eFA incorporation, the effect of eFA supplementation was also tested. To start with, cultures were supplemented with C16, as being the most naturally abundant FA reported in *Synechocystis salina* LEGE 06099 (Reis et al., 2020). The impact on

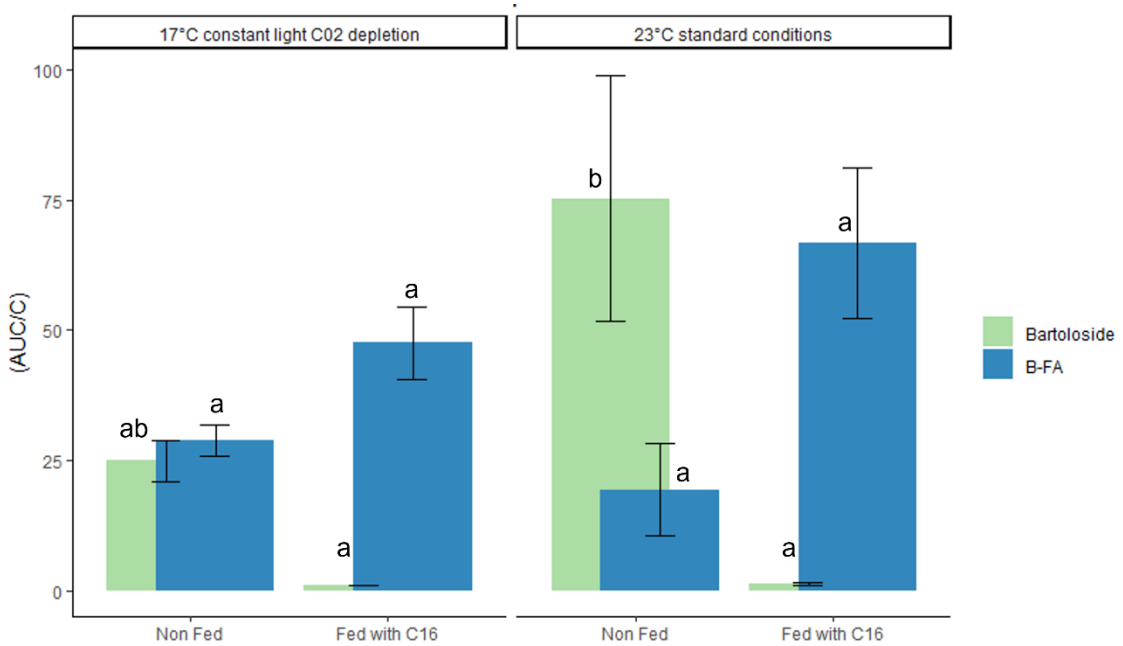

Figure 11 - *S. salina* 06099 B-FA and Bartoloside A quantity while cultures were grown with constant light supply and CO_2 deprivation, for 15 days at 17°C. Standard conditions were grown at 23°C. Growth experiments were performed in triplicate. The data represent the mean ± standard deviation (SD). The LC-MS analysis was performed on Xcalibur where respective area under the curve (AUC) was extracted for each mass. AUC was then normalized in AUC per cell (AUC/C). Same colored bars that do not include the same letter represent a significant statistical difference between each other.

those conditions at 17°C was investigated as it is closer to the temperature of the natural habitats of *S. salina* 06099 (sampled along Portugal's Coast). Strains growing at 23°C were chosen as the control condition, as not many differences were observed between growth at 23°C and 30°C (10% for Bartolosides and 2% for B-FAs - Annex, Table 3 and

6), while against 17°C both differ significantly more (~50% for Bartolosides and ~18% for B-FAs – Annex, Table 1 and 4) except for B-FA C2 production (Figure 8 and 9) which mostly varies wildly between days and temperatures. Based on the observed control data, the posterior experiments were conducted within 15 days of growth, as again, not significative differences were observed in B-FA composition between the different growth time points, except for B-FA C2 production (Figure 9 and 10). Cultures were grown either - at 17°C with CO_2 depletion (not total) or - at 17°C with CO_2 depletion (not total) and a constant light supply, both cultures were grown alongside a control culture at 23°C under the usual 16/8h light/dark cycle and normal room CO_2 flow. At all temperatures and under all conditions, half of the cultures were supplemented with C16 FAs (Figure 11 and 12). Results are consistent with previous feeding data obtained in the lab (Reis et al., 2020): upon FAs supplementation, and at both temperatures, independently of light and CO_2 conditions, bartoloside level is decreasing in favor of a proportionally consequent B-FAs increase. However, at 17°C, under constant light and CO_2 depletion, the trend observed in Figure 9 (higher production of bartoloside at lower temperature) is reversed, as a higher amount of bartoloside is observed at 23°C under normal conditions. This might be explained by the fact that under light and CO_2 stress, cells need to mobilize their energy for other metabolic functions and thus less resources are available for bartoloside production. However, it is still unexpected to observe a similar amount of bartoloside and B-FA without FAs supplementation under those conditions. Based on the data obtained and used literature no plausible hypothesis for this behavior has been built.

An additional culture subjected to only CO_2 depletion (Figure 12) was grown. When compared with the previous culture (Figure 11), it is possible to contrast the influence in B-FA production caused by CO_2 depletion, or constant light (or both).

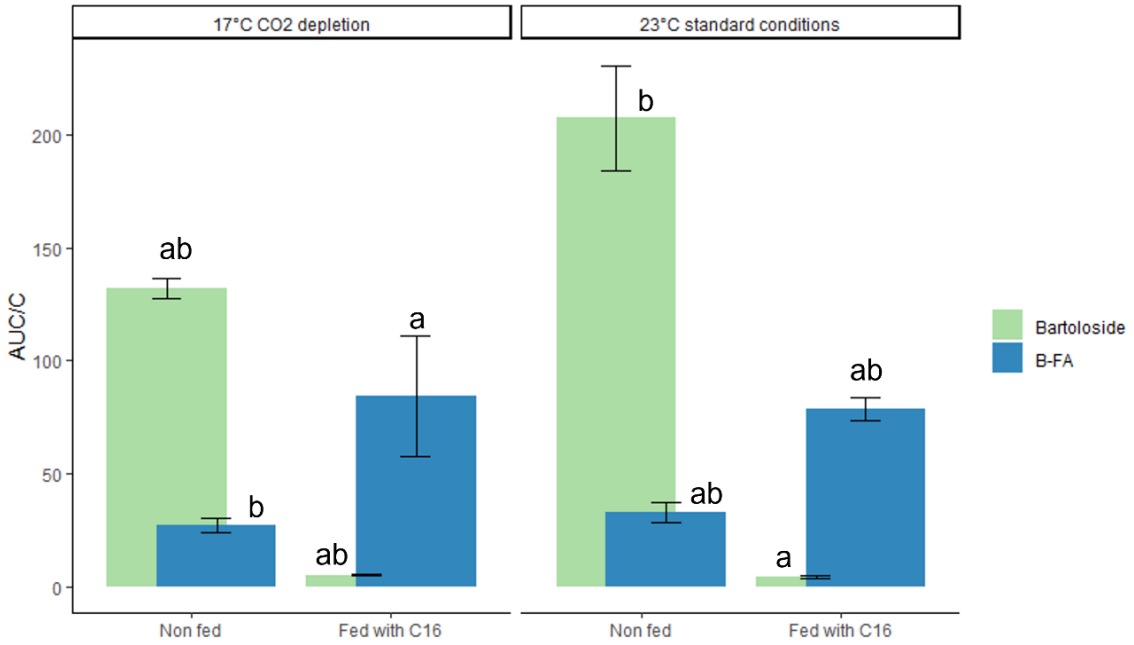

Figure 12 - *S. salina* 06099 B-FA and Bartoloside A quantity while cultures were grown with CO_2 deprivation during 15 days at 17°C. Standard conditions were grown at 23°C. Growth experiments were performed in triplicate. The data represent the mean ± standard deviation (SD). The LC-MS analysis was performed on Xcalibur where respective area under the curve (AUC) was extracted for each mass. AUC was then normalized in AUC per cell (AUC/C). Same colored bars that do not include the same letter represent a significant statistical difference between each other.

Comparing the groups defined by temperature and condition (CO_2 depletion), in the Bartolosides, significant differences were found globally (Kruskal-Wallis test, chi-squared= 9.46; df = 3, p=0.024 Annex, Table 8), while the same was true for the B-FAs (Kruskal-Wallis chi-squared = 9.359, df = 3, p-value = 0.025 Annex, Table 9). While the same is true for the previous experiment (Figure 11) (Kruskal-Wallis test, chi-squared= 9.4615; df=3, p= 0.02374 Annex, Table 10, and Kruskal-Wallis test, chi-squared= 8.7436; df=3, p= 0.0329 Annex, Table 11).

The bartoloside level and respective B-FA follow the same trend as Figure 11 as when only CO_2 is depleted from the culture, at 17°C (Figure 12): again, a lower amount of bartoloside is observed at 17°C when compared to 23°C. This indicates that only CO_2 depletion is enough to reverse the tendency of higher amount of bartolosides at lower temperature (Figure 9), but that a constant light might influence this tendency even more. The high error bar on the bartoloside production at 23°C without FA supplementation (Figure 11) does not allow to conclude if CO_2 depletion alone or if the light stress participate equally as for the observed decreased amount of bartoloside A at 17°C compared to 23°C. It can only be safely assumed that limiting CO_2 has a negative impact

on bartoloside production. However, even if bartoloside production is lower, B-FA production seems remain constant in non-fed cultures subjected to the experimental conditions, which could indicate that B-FA production is not affected in the same manner as bartoloside production under those stress conditions. On the other hand, no significant increase of B-FA was observed under either stress conditions, which did not allow to confer any particular role of B-FA under stress conditions.

The composition of FAs in B-FAs under all considered stress conditions was considered

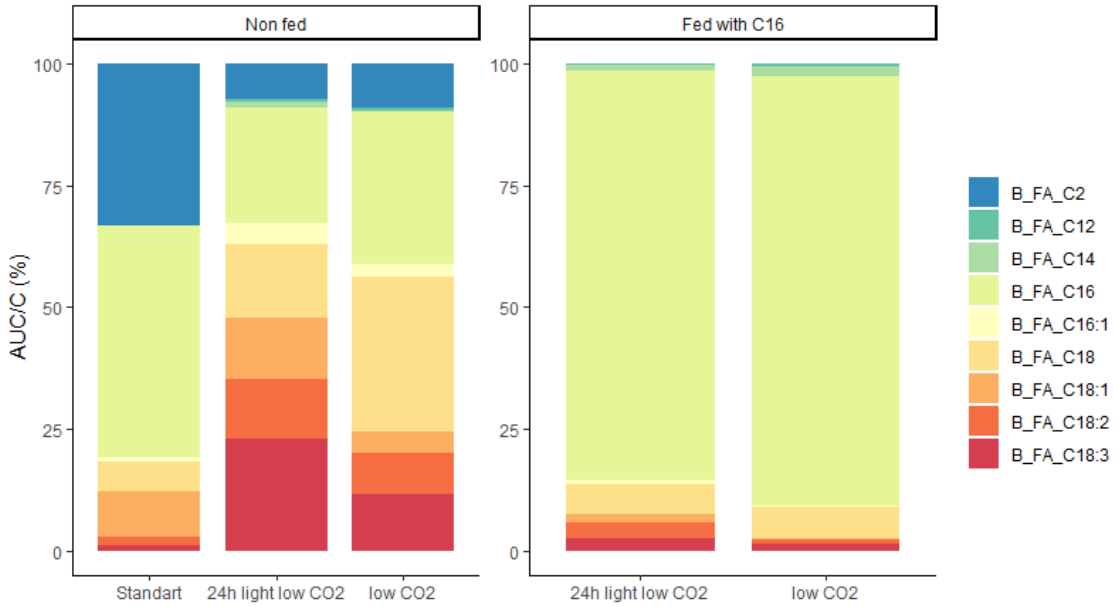

Figure 13 - Proportion of B-FAs A in *S. salina* 06099 culture grown at 17 °C under constant light and CO_2 depletion vs CO_2 depletion culture conditions, between non-fed conditions and between C16 feeding conditions. Standard condition grown at 23°C as a control group. Growth experiments were performed in triplicate, The LC-MS analysis was performed on Xcalibur where respective area under the curve (AUC) was extracted for each mass. AUC was then normalized in AUC per cell (AUC/C). Statistical analysis was done by permutational multivariate analysis of variance (PERMANOVA) and applied to the data using each of the B-FA types as response variable, while using the combinations of temperature and conditions as grouping factor (strata).

- light and CO_2 depletion, and after C16 supplementation.

The model was globally significant ($p < 0.001$) and all the combinations defined by the grouping factor were also significantly different from each other (Annex, Table 7).

Again, it can be observed the opposite trend towards unsaturated FAs when against the one observed under the control conditions (Figure 13), as a higher proportion of unsaturated B-FAs is observed at 17°C under stress conditions.

Short chain B-FA and particularly C2 is observed to be way less abundant after both light and CO_2 stress, than in the standard conditions. As the cell are stressed, and as C2 can be precursors of many other metabolic biomolecules, they might be required for other cellular metabolic reactions.

Additionally, unsaturated B-FA are shown to be present in a higher % under constant light exposure with C18:3 B-FA being the most abundant whilst under only CO_2 depletion,

saturated B-FAs like C18 B-FA are more prevalent. In *A. variabilis* it was reported that a drop in temperature leads to accumulation of polyunsaturated FAs, mainly C18 while exposed to light, meanwhile in a dark condition an accumulation of C16 was observed instead (Mironov et al., 2012, Cuellar-Bermudez et al., 2015, Los and Mironov, 2015). And in Synechocystis sp. PCC 6803, high light stress has been linked to several responses – faster rate of turnover of PSII, a decrease of light harvesting capacity, development of PSII protection mechanism, upregulation of general protection components and regulation of carbon and nitrogen assimilation (Muramatsu and Hihara, 2012). In relation to CO_2 depletion, it has been observed that cells grown with low carbon use their remaining intracellular carbon to mainly support biosynthesis, such as amino acids (Burnap et al.,2015). Additionally, some correlation was observed between low CO_2 and an increase in polyunsaturated FA production in algae (Cuellar-Bermudez et al., 2015) but it remains unaccounted for in cyanobacteria.

It seems that under light stress, B-FA production behaves the same way as other observed in lipid FAs that are produced in cyanobacteria while under high light stress, as polyunsaturated FAs (mainly C18) are the most common in both the used of constant light condition and high light in that regard (Figure 13). Still, high light stress is different than our 24-hour constant light condition, which means these effects cannot be concluded for certain.

When comparing fed with non-fed, an expected massive C16 incorporation in B-FAs was observed, and it seems that the other FAs remains in the same proportions as for the corresponding non fed condition.

Taken together, those results suggest that B-FA could have a role in storage/recycling of the basal pool of FAs present in the cell. Additional to its eFAs incorporation role, the Aas has been shown to also be responsible of cellular FFAs recycling. Hence, when FFAs would be released into the cell from membrane lipids or from other FA containing biomolecules, the Aas is responsible for their re-activation and re-incorporation (into other membrane lipids, neutral storage lipids, alaka(e)nes, FASII, etc.) (Kaczmarzyk and Fulda, 2010, Currie et al., 2010, Kaczmarzyk, 2008). Thus, a new hypothesis that BrtB could also possess this additional role of FFA recycling surged. This could be linked to membrane lipids FAs type remodeling in accordance with temperature, where B-FA

could be used as a storage of the lipids hydrolyzed FAs. Thereby a new a complementary analysis present in the figure below (Figure 14) was drawn.

A search for B-FA was also conducted in the extra cellular medium, but no B-FAs were

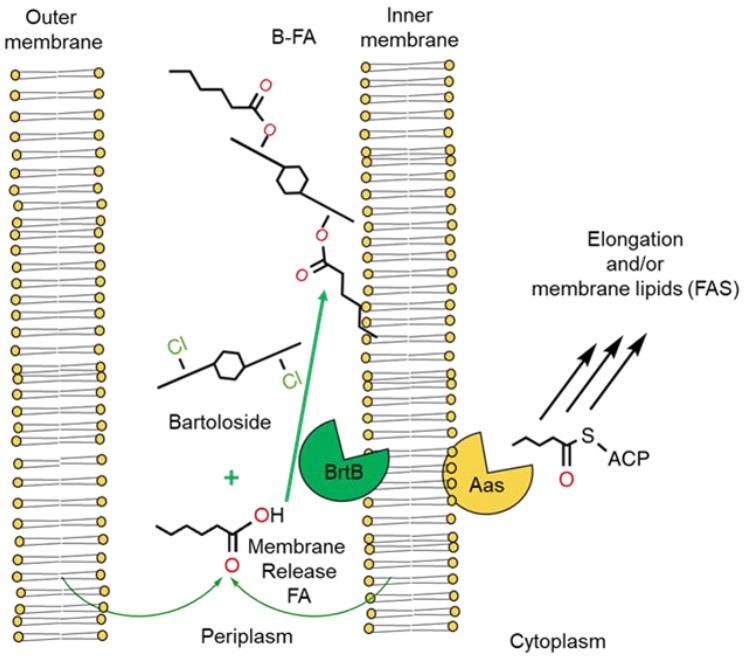

Figure 14 – Proposed representation of a new putative role for BrtB activity in FA recycling. B-FAs might be involved in a FFA recycling as demonstrated by the Aas system. The localization of all the pathway effectors is not yet determined however, BrtB is predicted to be membrane bound and was found to act prior/instead of the Aas in labelled FAs supplementation experiments.

detected with the extraction methods used. This indicates that B-FAs are not secreted outside the cell. To investigate our hypothesis further, and to elucidate any other possible Eco-physiological role, more test more conditions could be realized to confirm B-FA utilization and production inside the cell. Other environmental changes that can affect lipid production can be used, such as pH modification (effect of B-FA on pH inside the cells), co-culturing could provide insight into possible fitness advantages against other cyanobacteria not in possession of this system, as well as highlight its disadvantages if there are any. Building a continuous culture could prove insightful, in that a closer environment to the natural one can be constructed and used to better study natural production of these products. According to our putative model (Figure 14), monitoring FFA levels and comparing them to B-FA production would be a step to dig deeper into our hypothesis.

2.4 - Hydrolysis of B-FAs

As stated earlier, previous supplementation experiments in the lab conducted with the heavy stable oxygen isotope ^{18}O, have shown that, in S. salina 06099, eFAs incorporation was happening through BrtB, being directly (without prior activation)

incorporated into B-FAs (Annex Figure 2). In the same set of data, labelled hydrolyzed B-FAs were found, from which the FAs would have been cleaved (Annex Figure 3). This indicates that most likely, another enzyme could be responsible for cleaving FAs from B-FAs, as happening with primary lipids, leading to a recycling of the FAs esterified with the bartoloside, possibly into FFAs. Enzymes reported to hydrolyze FAs from lipids in cyanobacteria are known to be lipases and esterases, both of which cleave ester bonds in aqueous media, resulting in FFAs further re-activated by the Aas. Lipases in particular are ubiquitous enzymes with considerable physiological significance and are known to catalyze the hydrolysis of triacylglycerols to glycerol and free fatty acids (Sharma et al., 2001). Thus, a lipase, esterase, or any new putative lipolytic enzyme could be responsible for this hydrolysis process. Based on this information, a search for the enzyme responsible for the hydrolysis of the esters in B-FAs was started, by looking for homologue enzymes of the Aas system described in PCC 6803. Only a few studies have investigated the putative genes and enzymes encoding such enzymes in Cyanobacteria. However, two homologues annotated in PCC 6803 were found. The first candidate gene was described as an enzyme responsible for FA hydrolysis, sll1969, encoding the Lipase A (LipA) in PCC 6803. To our knowledge, LipA characterization has never been reported. Yet, some studies correlated LipA deletion and/or overexpression by a concomitant respectively decrease or increase of FFAs amount. Moreover, the experiments suggested this should not be the only candidate for FFAs release from lipids in PCC 6803 (Gao et al., 2012, Eungrasamee et al. 2019, 2021). A very recent study reported another second putative lipase, encoded by the gene sll0482, which was denominated as the protein Lipase 0482 (Lip0482). Though, neither the gene sll0482 nor its product have yet been subject to genetic or biochemical studies (Kojima et al. 2021). Both of those enzymes were found to possess homologues in S. *salina* 06099 genome, each sharing more than 90% identity (geneious) with the respective PCC 6803 homologue.

It is intended to test these lipases on extracted B-FA, to determine if they would be capable of hydrolyzing B-FA, or if any other additional putative lipase was yet to be discovered. To study these lipases, an heterologous expression is of the genes is first performed in E. coli. Two pET28a vectors containing each one of the lipases gene were engineered. The cloning of the two lipases in E. coli competent cells was found to be successful. Afterwards it proceeded to the testing of the expression of the corresponding proteins in small scale cultures of E. coli. As any expression study of homologues of LipA and Lip0482 could not be found, it was decided to base the conditions on previous experience of the Aas and ACP expression in E. coli – in both IPTG concentration (0.3 mM) and temperature of expression. The protein was not found to present in any

membrane domain (TMHMM-2.0, SignalP). However, as many lipases can be usually found attached to the membrane (Javed et al., 2018), both the soluble and insoluble fractions were collected. Cultures were grown at two different temperatures, one at 37°C for 4 hours, while another was grown at 20°C over-night (ON). Growth after induction at 37°C for 4 hours was found to express the highest number of proteins, and it was easy to observe both lipases expression by SDS-PAGE (Figure 15). However, the bands that migrated at the expected lipases size (LipA 25 kDa, Lip0482 (45 kDa) were found to be in the non-soluble fractions, indicating that our proteins are probably either membrane attached, membrane included or non-soluble.

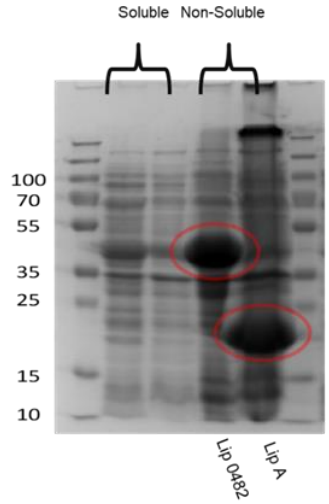

Figure 15 - SDS-PAGE gel of LipA (25 kDa) and Lip0482 (45 kDa) showing both soluble and non-soluble fractions upon small scale growth and cell lysis. Cultures shown in the gel were grown at 37°C for 4 hours. Gel was stained using Coomassie for 1 hour. Both lipases show in the non-soluble fraction.

The next steps will be to purify the proteins from a large-scale culture, from the non-soluble fractions, first with a membrane prep, and if not successful with a denaturation and refolding protocol, after which an enzymatic assays would be performed to test both lipases on their capability for the hydrolyzation of the FA in B-FAs. If unsuccessful, we will first look bioinformatically for a third putative enzyme, by comparing the genomes of BrtB containing strains to the close relatives that do not contain BrtB.

3 - Conclusions and perspectives

It is currently known that the Aas system plays an important role in eFA incorporation in cyanobacteria, which has led to hypothesis that the newly discovered BrtB system might play a similarly important role. The experiments showed that B-FA composition is highly linked to FA feeding and is affected by external environmental conditions (temperature, light, CO_2), as was previously known to be the case for membrane lipids. The B-FAs and their corresponding bartolosides, due to their high abundance, should play an important cellular role which seems to be linked to environmental conditions. The data could not yet be linked with any conclusion towards their role, even if, from the results, it seems to be more directed towards a structural and FFAs storage role. Thus, it would be interesting to test whether they provide fitness to their host or not, in certain conditions.

Currently only a few model strains are genetically engineered and used for further natural product discovery, biofuel production and so on. If no KO were successfully engineered in the present study, there will be further attempts to manipulate *S. salina* 06099. This would eventually prove useful not only to the continuation of this project in the future, but also to the cyanobacterial community.

Overall, when success is achieved in characterizing this system, a new pathway would be added to the understanding of cyanobacteria FA metabolism, as well as cyanobacteria adaptation to its environment.

Lastly, there are plans to characterize at least two new lipases, which could shed more light on the BrtB system, but will also be regarded as important tools by the biofuel community and industry, of which are constantly looking for new enzymes and advance knowledge and understanding of FA metabolism and their effects on FFA production and/or alka(e)ne production.

4 - Materials and Methods

4.1 - Cyanobacterial culture conditions

The strains used in that study are the unicellular cyanobacterium *Synechocystis salina* LEGE 06099 (*S. salina* 06099), a marine strain from the LEGE culture collection (LEGEcc), and *Synechocystis sp.* PCC 6803 (PCC 6803), a unicellular model freshwater strain from the Pasteur culture collection (PCC). The first one was reported to possess the brt gene cluster and to produce a high amount of bartolosides (Reis et al., 2020), the second one does not possess the brt gene cluster nor does it produce bartolosides. Both contain the Aas activation pathway. The third strain used in that study is an engineered *Synechocystis sp.* PCC 6803 strain in which the Aas gene was knocked out (KO): PCC 6803 *Aas*.

Cultures of *S. salina* 06099 were grown in Z8 medium supplemented with 25 g/L sea salts (Tropic Marin) from 17°C to 30°C according to the experiments, the optimal growth being 30°C, under a 16:8h light/dark cycle with a light intensity of 55 µmol m^{-2} s^{-1} and shaking at 100 revolutions per minute (rpm).

The two PCC 6803 strains were grown in Z8 medium, at 30°C with 55 µmol m^{-2} s^{-1} light intensity and shaking at 100 rpm in a 16/8h light/dark cycle. For every experiment the starting optical density (O.D.) was set between 0.01-0.02 (λ=750 nm).

4.2 - Growth curve Assay

150 mL of cultures were grown in Z8 medium supplemented with 25 g/L sea salts (Tropic Marin), at different temperatures (17°C, 25°C and 30°C) under a 16:8h light/dark cycle, a light intensity of 55 µmol m^{-2} s^{-1}, shaking at 100 rpm for up to 50 days. Cultures grown at 25°C and 30°C were grown in triplicate, cultures grown at 17°C were grown in duplicate. Cultures were inoculated with a starting O.D. of 0.02 (λ=750 nm). Their O.D. was periodically measured, 10 to 25 mL according to the cell density were sampled at the same time for further biomass extraction and LC-MS analysis. The O.D. measurement and the samples collection were realized at day 5, 10, 15, 20, 27, 34 and 50. The O.D. was then further converted to cell amount for cell normalization in further analysis.

4.4 - Cell normalization

S. salina 06099 cultures were first prepared with a gradient of increasing O.D., from 0.301 to 1.862 (7 cultures). A drop of the cultures was loaded into a Neubauer counting chamber. According to the size of the cells, small squares of the chamber were used to count the number of cells per square, repeated for each O.D. 6 to 7 times, and were additionally multiplied per O.D.. This number was then transformed into number of cells per mL and averaged. With the O.D. and the number of cells per mL a calibration line was built, and its equation was used to obtain the number of cells for each O.D. in the collected data of S. salina 06099.

The further described area under the curve (AUC) data that are obtained through the program Xcalibur coming from LC-MS analysis and correlated to bartolosides and B-FA. Using both cell number and AUC, cell normalization was achieved using AUC per cell (AUC/C).

4.5 - C16 supplementation experiments

For the first reported feeding experiment (Fig 11), cultures used for feeding experiments were grown in 60 mL Z8 medium with 25 g/L sea salts, at two different temperatures, 17 °C and 23 °C, in triplicate, with an initial O.D. of 0.02.
Cultures that were grown at 23 °C under a 16/8h light/dark cycle, under light intensity of 55 µmol m^{-2} s^{-1}, shaking at 100 rpm.
The cultures at 17 °C were grown under constant light (55 µmol m^{-2} s^{-1} without dark period), and without aeration (no external source of CO2 was provided, except as when the door of the incubator would be open for culture sampling).

For each temperature, triplicates were grown without FA supplementation, and additional triplicates were grown by supplementing C16 palmitic FA at a final concentration of 0.4 mM at the 9th day of growth. The palmitic acid was stored in 50% DMSO at a stock concentration of 500 mM. Not more than a final concentration of 1% of DMSO was added to the fed cultures. Sampling for further biomass extraction and O.D. measurement was conducted at day 10 (40 mL was sampled), and at day 15 (the remaining 15 mL). After each sample was collected, a centrifugation step was performed at 8899 x g at room temperature, and the supernatant kept at -20°C for extracellular extraction.

For the second reported feeding experiment (Fig 12), all the growth and feeding conditions were similar. Cultures were grown in 160 mL Z8 medium with 25 g/L sea salts, at 17 °C and 23 °C, in triplicate, with an initial O.D. of 0.02.

Cultures were grown at both temperatures under a 16/8h light/dark cycle, under light intensity of 55 µmol m^{-2} s^{-1}, shaking at 100 rpm. At day 10 of the experiment there was a first sampling (45mL) and at day 15 there was a second sampling (45mL) of the cultures. After each sample was collected, a centrifugation step was performed at 8899 x g at room temperature, and the supernatant kept at -20°C for extracellular extraction.

4.6 - Organic extraction

Organic extraction (OE) of the intracellular compounds:

Biomass sampled from the growth curve and C16 supplementation experiments was centrifuged at 4000xg, further washed with one volume of double distilled water (DDW) and centrifuged again at 4000xg. The pellet stored at -20°C over-night (ON), after which it was freeze-dried and stored at -20 °C until further organic extraction.
The organic extraction was carried through repeated percolation steps using a mixture of CH2Cl2/MeOH (2:1, v/v), at room temperature. Solvent volume was adjusted according to the sample size. The solvent was filtered (through 90mm filter papers first, and a second time through Minisart RC 4 0.2 µm syringe filters) and removed *in vacuo* with the extract stored at – 20°C until further use.

Organic extraction of the extracellular compounds:

After the first above-described step of centrifugation (OE of the intracellular compounds), the remaining supernatant was frozen at -20°C until further use.
The extraction was carried out at room temperature using Acetyl Acetate ($C_4H_8O_2$) in a 1:1 ratio with the sample. The mixture was set to shake for 15 minutes, after which the Acetyl Acetate was removed from the top of the mixture (the acetyl acetate does not mix with the sample after shaking). This step was repeated at least one more time. The resulting solvent was filtered and removed *in vacuo* and the extract stored at -20 °C until further use.

4.7 - LC-HRESIMS analysis

LC-HRESIMS and LC-HRESIMS/MS analyses were performed on an UltiMate 3000 UHPLC (Thermo Fisher Scientific) system composed of an LPG-3400SD pump, WPS3000SL autosampler, and VWD-3100 UV/vis detector coupled to a Q Exactive Focus Hybrid Quadrupole-Orbitrap mass spectrometer controlled by Q Exactive Focus Tune 2.9 and Xcalibur 4.1 (Thermo Fisher Scientific).

HRMS data were obtained in Full Scan negative mode with a scan range of m/z 150-2000, with a capillary voltage of H set to −3.8 kV and the capillary temperature to 300°C. Sheath gas flow rate was set to 35 units.

OE extract that was stored at -20°C was defrosted, and 1 mg/mL of compounds were transferred into LC-MS vials in Methanol (MeOH), after being filtered. During the LC-HRESIMS analysis, separation was performed in a Luna C18 column (100 × 3 mm, 3 µm, 100 Å, Phenomenex). A mixture of MeOH/H2O 1:1 (v/v) with 0.1% formic acid (eluent A) and isopropanol (IPA) with 0.1% formic acid (eluent B) were used as mobile phase, under a flow rate of 0.4 mL/min.

10 µL injection of crude extracts of biomass were analyzed by LC-HRESIMS using a gradient from at 9:1 to 1:4 eluent A/eluent B in 3 min and held for 28 min before returning to initial conditions.

4.8 - HRESIMS/MS analysis

MS/MS parameters for the LC-HRESIMS/MS analysis were resolution of 35000, with a 1 m/z isolation window, a loop count of 3, AGC target of 5×104 and collision energy of 35 eV.

4.9 - Data analysis

Data obtained through LC-MS and MS/MS were looked at through the program Xcalibur (Annex Figure 5, 6). Exact masses of the compounds and of the fractionated compounds were obtained through ChemDraw (Annex Table 12). Data were then organized and processed in Excel and then R.

4.10 - Knock-outs of the Aas and BrtB genes in S. salina 06099

4.10.1 - Plasmid production:

To knock-out (KO) the Aas and the BrtB gene separately in two different S. salina 06099 strains, natural transformation was envisioned and tried. A pBlueScript plasmid was used to perform the KO by homologous recombination and incorporation of a Kanamycin resistance cassette instead of the gene of interest, surrounded by two complementary fragments of the upstream and downstream part of either the Aas or the BrtB gene. The plasmids were constructed and verified by sequencing earlier in the laboratory. Upon my arrival, the plasmids were refreshed by performing a heat shock transformation into E. coli XL1 strain. To perform the heat-shock, 50 µL E. coli XL1 competent cells were unfrozen on ice, 5 µL of the previous plasmid (containing the up and downstream

fragment complementary to either the Aas or BrtB) was added to them and put on ice for 20 min, the heat shock was then performed for 45 sec at 42°C. Cells were transferred to ice for 2 additional minutes, and then placed at room temperature for 2 additional minutes. 250 µL of SOC medium was further added to the cells, after which the cells recovered for 30 min to 1h in a 37°C incubator shaking at 200 rpm. 100 µL was plated on Kanamycin LB plates and incubated over-night (ON) at 37°C.

A single colony was picked and put to grow in 5 mL of LB containing 5 ug of Kanamycin for approximately 18h. Cells were then centrifuged at 13000 x g, and the plasmids further purified by the mean of a NZYMiniprep (NZYTech) kit. Fresh plasmids were stored at -20°C. Two (for both Aas and BrtB KO) glycerol stock of the XL1 transformed cells were kept at -80°C.

4.10.2 - Natural transformation:

50 mL of fresh culture of S. salina 06099 was grown in BG 11 with 2.5 g/L of sea salts with a starting O.D. of 0.01 to a final O.D. of ~0.5, the culture was then concentrated to a final O.D. of 2.5 through centrifugation (3000 x g) and resuspension steps.

Then, three Eppendorf with 500 mL of culture were prepared. One as a negative control, the two others for each of the KOs. Plasmid was added to each of the Eppendorf, except for the negative control, to a final concentration of 1 to 10 ug/mL. The three tubes were then left to incubate for ~6 hours under 50 µmol m^{-2} s^{-1} light shaking at 100 rpm, after which, the contents of the Eppendorfs were spread on a cell culture membrane placed inside a BG 11 agar plate with 2.5 g/L of sea salts and incubated at low light at 30 °C for 48 hours.

Once the 48h were past, the membranes were cut into thirds for the control and in half for the KOs, one third was left in the control plate with no antibiotics, and the other thirds were plated in BG 11 agar 2.5g/L salt plates with 10 ug/mL Kanamycin and another with 10 ug/mL Neomycin (only the latter two for the KOs). Any resulting colonies would be picked and replated or simply the membrane would be transferred into a higher concentration antibiotic BG 11 agar plate, until full chromosomal segregation of the transformed plasmid was achieved.

For confirmation of the incorporation and segregation of the Kan cassette instead of the Aas or BrtB gene onto each chromosome copy in LEGE 06099 transformed cells, colony PCRs were performed on colonies grown on the previously described kanamycin plates used for segregation. Colonies were touched with a loop, and the loop further inserted into the PCR mix. The conditions of each PCR are shown in the present tables:

Table 2 - Primers used for the colony PCR described in chapter 2.1.1 (Fig 5)

Gene/cassette	Localization	Sequence
BrtB	**Forward**	**GAGTTGGGGATCGAGATCG**
	Reverse	**GCGGAATGTGTTGAGTTCGC**
Kanamycin	**Forward**	**AAACTGCAGTGAGGTCTGCCTCGTGAAGAA**
	Reverse	**AAACTGCAGAAAGCCACGTTGTGTCTCAAA**
Aas	**Forward**	**ATTACCGGTTCATCGCTGACCAAG**
	Reverse	**TATAGAAAGGTTTGGGTCATCATGC**

Table 3 - Settings used for the colony PCR described in chapter 2.1.1 (Fig 5). Annealing temperatures and duration differed for each pair of primer: Y represents 30 seconds for the primer used for the amplification of the Kanamycin cassette and the BrtB gene, 50 seconds for the primer used for the amplification of the for Aas. X is 67°C for BrtB and Aas amplification, 62°C for Kanamycin amplification.

Step	T (°C)	Time	Cycles
Initial Denaturation	98	3 min	1
Denaturation	98	10 s	30/35
Annealing	X	Y s	
Extension	72	40 s	
Final extension	72	2 min	1
Hold	4	Hold	------

Components	Volume (100 µL)
Q5 High-Fidelity 2X Master Mix, Biolabs	50 µL
Forward primer	5 µL
Reverse primer	5 µL
DNA	Touch w/ colony
DDW	40 µL

Colonies found segregated or partially segregated were re-plated on higher or same concentration BG 11 Kan plates.

4.11 - Chemical Knock-out optimization assays

The cyanobacteria strains used for the assays were described above: S. salina 06099, PCC 6803, PCC 6803 Aas KO, and grown as written previously.

Assays used a starting O.D. of ~0.1, Z8 media (according to strain needs), cerulenin, FA mixes (C2, C6, C10, C12, C14, C16, C18) and the inhibitor C10-AMS [5′O(Ndecanylsulfamoyl)adenosine].

Tests were performed in 96 wells plates at 23°C shaking at 100 rpm, in triplicate, with a total volume of 200 uL per well. All OD were measured at an absorbance of 750 nm, using a microplate reader (BioTek Cytation 5 Cell Imaging Multimode Reader, Agilent). Concentrations were tested from: 0.5 nM to 1 µM (AMS-C10), 5 µM to 100 µM (cerulenin), 50 µM to 1 mM (FA mix).
Larger scale assay: experiments were conducted in a total volume of 4 mL (using a 10 mL Erlenmeyer), with a starting O.D. of ~0.1 and grown at 23°C shaking at 300 rpm. Concentrations from 0.5 µM to 100 µM of AMS-C10 were tested. Every test was repeated in triplicate except F and G.

4.12 - Labelled C12 supplementation and AMS-C10 inhibition assay

PCC 6803 was supplemented with 500 mM of labelled deuterated C12 FA and 1.67 µM of AMS-C10.

This assay was conducted under 4 different conditions, for 2 time points (3 days and 8 days): A control condition fed with C12 non-labelled FA, a second control condition fed with C12 labelled FA, a third condition supplemented with non-labelled C12 and AMS-C10 and a final fourth condition supplemented with labelled deuterated C12 FA and AMS-C10 (8 total). Cultures had an initial O.D. of ~ 0.1 and were grown in 50 mL culture flasks in 25 mL Z8 media. Feeding was done in pulses (2 times) of 35.55 µL of AMS-C10 4.7 µM with a final concentration 1.67 µM AMS-C10, and 12.5 µL of the labelled and non-labelled C12 FA (500 mM) were added 1 day later. The feedings were done for 3 and 8 days, we added the labelled FA at day 1, and the AMS-C10 from day 0, then we added again, 2 days later the same amounts.

The cultures were then collected, the biomass was centrifuged at 4000xg and washed with DDW, and frozen at –20°C for a day, and promptly lyophilized and stored again at -20°C.

OE of the compounds was carried out as written in above on the extraction of intracellular compounds. Data were analyzed through Xcalibur and Excel.

4.13 - Statistical analysis

All the statistical analyses were performed with R software (R Core Team, 2022). For the analysis of variance (ANOVA), the functions *lm* and *shapiro.test* were employed from package *stats*, as well as *Anova* and *leveneTest* from package *car*.

In this analysis the function *glht* from package *multcomp* was also employed for the Tukey test in the pos-hoc pairwise comparisons.

For the permutational analysis of variance (PERMANOVA) the function PERMANOVA was employed, from the *homonym* package, using Bray-Curtis as distance measure. For the Kruskal-Wallis test the *kruskal.test* function was used, from package *stats*, and for the Nemenyi test in the post-hoc pairwise comparisons we recurred to the function *kwAllPairsNemenyiTest*, from package *PMCMRplus*.

4.14 - Cloning of known lipase of *S. salina 06099* in *E. Coli*

A Blast (gene to protein, in geneious software) was performed between PCC 6803 lipases (sll1969 and sll0482) and S. salina 06099 genome. Two homologues protein were found, with each more than 95% homology.

PCR was used for the cloning of those two different lipases. Cyanobacterial genomic DNA (gDNA) was extracted with the NZY Plant/Fungi gDNA Isolation kit following the manufacturer instructions, and further used for PCR amplification. The constructs were cloned into a pET28a plasmid, containing a His-Tag for subsequent purification and a Kanamycin resistance cassette for selection.

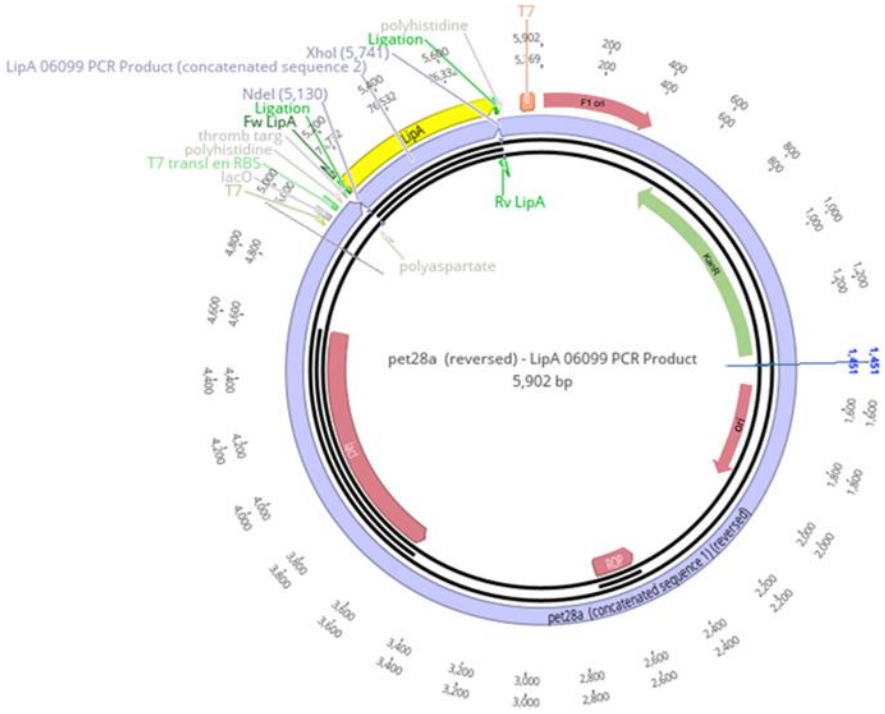

Figure 16 - The pET-28a (+) vector carries an N-terminal His-Tag/thrombin/T7-Tag configuration, the gene of interest (LipA) between Nde1 and Xhol1 restriction enzymes sites, f1 origin(f1), T7 promoter, kanamycin resistance (Kan R), pBR322 replication origin (ori), LacI coding sequence, rop protein sequence.

Table 4 - Primers used for the cloning of both lipases of interest into a pET-28a vector

Protein	Enzyme	Localization	Sequence
Lip A	**NdeI**	**Forward**	**tgatcCATATGGTGGCAGAAGTTCCAGACC**
	XhoI	**Reverse**	**atgatCTCGAGTCAGGTCAAAGGTTGAGCC AAAG**
Lip 0482	**NdeI**	**Forward**	**gtactCATATG GGAATCTTTAACCGCAGAAGAC**
	XhoI	**Reverse**	**aatatCTCGAGTCAAACGGCGGCGATG**

4.15 - PCRs

PCRs were performed using the Q5 High-Fidelity 2X Master Mix (New England Biolabs), and 5 to 10 µL of the resultant reaction further run into a 1.2% agarose gel under 90V for 35min. The first PCR was performed in 50 µL final volume divided into five 10 µL volume tubes to test different primers annealing temperature (from 58°C to 67°C). The second PCR product was then performed in 50 µL final volume and further cleaned with a PCR purification kit (NZYtech).

Table 5 - PCR program and mix preparation for lipase cloning

PCR mix preparation	Program
Q5 master mix 25 µL	98°C for 30 sec
Primer Fw 2.5 µL from 1/10 dilution stock	98°C for 10 sec
Primer Rev 2.5 µL from 1/10 dilution stock	64°C (LipA) or 67°C (Lip0482) for 30 sec
DNA 1 µL (99 ng/uL)	72°C for 18 sec (LipA) or 35sec (Lip0482)
DDW 19 µL	72°C 2 min

4.15.1 - Restriction enzyme digestion

For the digestion, the PCR product was cleaned with the NEbiolabs kit.

1 µg of plasmid was digested by NdeI (1µL) and XhoI (1µL) (Biolabs), as well as 1 µg (for each tube) of pET28a (99 ng/µL of initial concentration), pET28a + LipA gene (63 ng/µL) and pET28a + Lip0482 gene (68 ng/µL). The reaction took place in a final volume of 50 µL, including 5 µL of buffer and the rest of DDW, incubated at 37°C for 1h.

Table 6 - Digestion mix preparation step for lipase cloning

1 ug of **Pet 28a**	1 ug of **LipA** PCR product	1 ug of **Lip0482** PCR product
1 µL of NdeI	1 µL of NdeI	1 µL of NdeI
1 µL of XhoI	1 µL of XhoI	1 µL of XhoI
5 µL of Cutsmart buffer	5 µL of Cutsmart buffer	5 µL of Cutsmart buffer
33 µL of DDW	27 µL of DDW	28 µL of DDW

4.15.2 - Ligation

Ligation was performed with the DNA fragments obtained through previous digestion into a pET28a plasmid using a T4 ligase at 4°C overnight.

Table 7 - Ligation mix preparation step used for lipase cloning

2 µL of DNA (of either LipA or Lip0482)
5 µL of pet28a
0.5 µL of ligase T4
1 µL of Buffer ligase
1.5 µL of DDW

4.15.3 - Transformation and selection

The XL1 E. coli competent cells were used for transformation with the obtained pET28a transformed with the LipA/Lip0482.
Transformation was performed by heat shock using 50 µL of the competent cells with 5 µL of the transformed plasmid. This was achieved by placing the cells for 30 minutes on ice, followed by 45 seconds at 42°C, and 2 more minutes on ice. After 2 minutes, 200 µL of SOC was added and the cells recovered at 37°C for 30 minutes to 1 hour. 100 µL of the obtained cells were plated on LB Kan plates of 50 µg/ml.

Once grown, some colonies were randomly picked to perform a miniprep plus digestion with NdeI/XhoI restriction enzymes to verify the transformation of the cells.

At the time of this experiment the nanodrop was not working, but we estimated that the plasmid concentration would not be lower than 20 ng/µL and digested 1 µg of plasmid.

4.15.4 - Small-scale expression

E. coli BL21 DE3 Rosetta competent strain was used for over-expression of the recombinant proteins, LipA and Lip0482. The competent cells were transformed as described above for XL1. From the plates, some colonies were picked for precultures growth in 5 mL LB medium (plus Kanamycin 50 µg/mL) and incubated overnight at 37 °C for 16-18 hours. 250 µL of preculture was then transferred into 25 mL TB medium (+Kanamycin 50 (25 µL of stock 50) and MgSO4 5 mM (125 µL of 1M stock). When reaching an O.D. (λ=600) of ~ 0.6, protein expression was induced by adding Isopropyl β-d-1-thiogalactopyranoside (IPTG) to a final concentration of 0.3 mM (12.5 µL of 1M stock) and incubated for 18-20 hours at 20°C and at 37°C, cultures were incubated for around 4 hours, both shaking at 200 rpm.

After protein expression, cultures were centrifuged at 4000 x g for 10 minutes, 4°C. Pellets were then resuspended in 300 µL of BugBuster (Merck), containing a final concentration of 0.5 mg/mL lysozyme (Sigma, stock 10 mg/mL). The suspension was incubated at 4°C for 5 minutes. 0.5 µL of Benzonase Nuclease (Merck) and 10 mM of MgSO4 (3 µL of 1 M stock) were added and the solution incubated again at 4°C for 5 minutes. The suspension was centrifuged at 17.000 x g for 15 minutes, 4°C. The soluble supernatant was collected, and the non-soluble fraction centrifuged again for 2 minutes. The supernatant was discarded and 300 µL of 2% SDS added to the non-soluble fraction. Finally, 20 µL of sample were mixed with 20 µL of 2x SDS loading buffer and SDS page run (4-20% Mini-PROTEAN TGX precast gel, BIO-RAD) for 10 mins at 80V whereafter the voltage was increased to 200V for around 40 mins. Afterwards distilled water was added to the gel for 15 minutes to remove residual SDS, and then replaced by Coomassie Blue G250 BioSafe (BioRad) (just enough to cover the gel) for about 1 hour while rocking. Next, the staining agent was removed, and water added again for a minimum of 1 hour (over-night for higher clarity).

5 - References

Afonso, T. B., Costa, M. S., Rezende de Castro, R., Freitas, S., Silva, A., Schneider, M. P., . . . Leão, P. N. (2016). Bartolosides E-K from a Marine Coccoid Cyanobacterium. *J Nat Prod, 79*(10), 2504-2513. doi:10.1021/acs.jnatprod.6b00351

Azim, Kamran & Shoukat, Khalida. (2009). Homology modeling of V. cholerae long chain fatty acid transporter FadL., Pak. J. Biochem. Mol. Biol., 42(4): 129-135

Bellefleur, M.P.A., Wanda, SY. & Curtiss, R. (2019) Characterizing active transportation mechanisms for free fatty acids and antibiotics in Synechocystis sp. PCC 6803. BMC Biotechnol 19, 5. https://doi.org/10.1186/s12896-019-0500-3

Berlepsch, S., Kunz, H.-H., Brodesser, S., Fink, P., Marin, K., Flügge, U.-I., & Gierth, M. (2012). The Acyl-Acyl Carrier Protein Synthetase from Synechocystis sp. PCC 6803 Mediates Fatty Acid Import. *Plant Physiol., 159*, 606-617. doi:10.1104/pp.112.195263

Büdel, B. (2011). Cyanobacteria: Habitats and Species. *2*. doi:10.1007/978-3-642-19106-0_2

Burnap, R. L., Hagemann, M., & Kaplan, A. (2015). Regulation of CO2 Concentrating Mechanism in Cyanobacteria. *Life (Basel), 5*(1), 348-371. doi:10.3390/life5010348

Chen, Z., Li, X., Tan, X., Zhang, Y., & Wang, B. (2020). Recent Advances in Biological Functions of Thick Pili in the Cyanobacterium Synechocystis sp. PCC 6803. *Front Plant Sci, 11*, 241. doi:10.3389/fpls.2020.00241

Cuellar-Bermudez, S. P., Aguilar-Hernandez, I., Cardenas-Chavez, D. L., Ornelas-Soto, N., Romero-Ogawa, M. A., & Parra-Saldivar, R. (2015). Extraction and purification of high-value metabolites from microalgae: essential lipids, astaxanthin and phycobiliproteins. *Microb Biotechnol, 8*(2), 190-209. doi:10.1111/1751-7915.12167

Currie, M. F., Persaud, D. M., Rana, N. K., Platt, A. J., Beld, J., & Jaremko, K. L. (2020). Synthesis of an acyl-acyl carrier protein synthetase inhibitor to study fatty acid recycling. *Sci Rep, 10*(1), 17776. doi:10.1038/s41598-020-74731-4

Eungrasamee, K., Incharoensakdi, A., Lindblad, P., & Jantaro, S. (2020). Synechocystis sp. PCC 6803 overexpressing genes involved in CBB cycle and free fatty acid cycling enhances the significant levels of intracellular lipids and

secreted free fatty acids. *Sci Rep, 10*(1), 4515. doi:10.1038/s41598-020-61100-4

Eungrasamee, K., Incharoensakdi, A., Lindblad, P., & Jantaro, S. (2021). Overexpression of lipA or glpD_RuBisCO in the Synechocystis sp. PCC 6803 Mutant Lacking the Aas Gene Enhances Free Fatty-Acid Secretion and Intracellular Lipid Accumulation. *Int. J. Mol. Sci. 22*(21), 11468.

Eungrasamee, K., Miao, R., Incharoensakdi, A., Lindblad, P., & Jantaro, S. (2019). Improved lipid production via fatty acid biosynthesis and free fatty acid recycling in engineered Synechocystis sp. PCC 6803. *Biotechnol Biofuels, 12*, 8. doi:10.1186/s13068-018-1349-8

Figueiredo, S. A. C., Preto, M., Moreira, G., Martins, T. P., Abt, K., Melo, A., . . . Leão, P. N. (2021). Discovery of Cyanobacterial Natural Products Containing Fatty Acid Residues*. *Angew Chem Int Ed Engl, 60*(18), 10064-10072. doi:10.1002/anie.202015105

Ford, A. K., Visser, P. M., van Herk, M. J., Jongepier, E., & Bonito, V. (2021). First insights into the impacts of benthic cyanobacterial mats on fish herbivory functions on a nearshore coral reef. *Sci Rep, 11*(1), 7147. doi:10.1038/s41598-021-84016-z

Gao, Q., Tan, X., & Lü, X. (2012). [Characterization of a key gene in membrane lipid cycle in Synechocystis sp. PCC6803]. *Sheng Wu Gong Cheng Xue Bao, 28*(12), 1473-1481.

Gombos, Z., Wada, H., & Murata, N. (1992). Unsaturation of fatty acids in membrane lipids enhances tolerance of the cyanobacterium Synechocystis PCC6803 to low-temperature photoinhibition. *Proc Natl Acad Sci U S A, 89*(20), 9959-9963. doi:10.1073/pnas.89.20.9959

Huisman, J., Codd, G. A., Paerl, H. W., Ibelings, B. W., Verspagen, J. M. H., & Visser, P. M. (2018). Cyanobacterial blooms. *Nature Reviews Microbiology, 16*(8), 471-483. doi:10.1038/s41579-018-0040-1

Ikeuchi, M., & Tabata, S. (2001). Synechocystis sp. PCC 6803 - a useful tool in the study of the genetics of cyanobacteria. *Photosynth Res, 70*(1), 73-83. doi:10.1023/a:1013887908680

Javed, S., Azeem, F., Hussain, S., Rasul, I., Siddique, M. H., Riaz, M., . . . Nadeem, H. (2018). Bacterial lipases: A review on purification and characterization. *Prog Biophys Mol Biol, 132*, 23-34. doi:10.1016/j.pbiomolbio.2017.07.014

Kaczmarzyk, D., & Fulda, M. (2010). Fatty acid activation in cyanobacteria mediated by acyl-acyl carrier protein synthetase enables fatty acid recycling. *Plant Physiol, 152*(3), 1598-1610. doi:10.1104/pp.109.148007

Kojima, K., Matsumoto, U., Keta, S., Nakahigashi, K., Ikeda, K., Takatani, N., . . . Aichi, M. (2021). High-Light-Induced Stress Activates Lipid Deacylation at the Sn-2 Position in the Cyanobacterium Synechocystis Sp. PCC 6803. *Plant and Cell Physiology, 63*(1), 82-91. doi:10.1093/pcp/pcab147 %J Plant and Cell Physiology

Kotai, J. (1972). Instructions for preparation of modified nutrient solution Z8 for algae.

Kufryk, G. I., Sachet, M., Schmetterer, G., & Vermaas, W. F. J. (2002). Transformation of the cyanobacterium Synechocystis sp. PCC 6803 as a tool for genetic mapping: optimization of efficiency. *FEMS Microbiology Letters, 206*(2), 215-219. doi:10.1111/j.1574-6968.2002.tb11012.x %J FEMS Microbiology Letters

Lang, I., Hodac, L., Friedl, T., & Feussner, I. (2011). Fatty acid profiles and their distribution patterns in microalgae: a comprehensive analysis of more than 2000 strains from the SAG culture collection. *BMC Plant Biology, 11*(1), 124. doi:10.1186/1471-2229-11-124

Leão, P. N., Nakamura, H., Costa, M., Pereira, A. R., Martins, R., Vasconcelos, V., . . . Balskus, E. P. (2015). Biosynthesis-assisted structural elucidation of the bartolosides, chlorinated aromatic glycolipids from cyanobacteria. *Angew Chem Int Ed Engl, 54*(38), 11063-11067. doi:10.1002/anie.201503186

Los, D. A., & Mironov, K. S. (2015). Modes of Fatty Acid desaturation in cyanobacteria: an update. *Life (Basel), 5*(1), 554-567. doi:10.3390/life5010554

Mironov, K. S., Sidorov, R. A., Trofimova, M. S., Bedbenov, V. S., Tsydendambaev, V. D., Allakhverdiev, S. I., & Los, D. A. (2012). Light-dependent cold-induced fatty acid unsaturation, changes in membrane fluidity, and alterations in gene expression in Synechocystis. *Biochim Biophys Acta, 1817*(8), 1352-1359. doi:10.1016/j.bbabio.2011.12.011

Muramatsu, M., & Hihara, Y. (2012). Acclimation to high-light conditions in cyanobacteria: from gene expression to physiological responses. *J Plant Res, 125*(1), 11-39. doi:10.1007/s10265-011-0454-6

Murata, N. (1989). Low-temperature effects on cyanobacterial membranes. *J Bioenerg Biomembr, 21*(1), 61-75. doi:10.1007/bf00762212

Nalley, J., O'Donnell, D., & Litchman, E. (2018). Temperature effects on growth rates and fatty acid content in freshwater algae and cyanobacteria. *Algal Res., 38*, 500-507. doi:10.1016/j.algal.2018.09.018

Pope, M. A., Hodge, J. A., & Nixon, P. J. (2020). An Improved Natural Transformation Protocol for the Cyanobacterium Synechocystis sp. PCC 6803., *Front. Plant Sci*. *11*. doi:10.3389/fpls.2020.00372

Raven, J., & Geider, R. (1988). Temperature and growth. *New Phytologist - NEW PHYTOL, 110*, 441-461. doi:10.1111/j.1469-8137.1988.tb00282.x

Raven, J. A., & Geider, R. J. J. N. P. (1988). Temperature and algal growth., *New Phytol., 110*, 441-461.

R Core Team (2022). R: A language and environment for statistical computing. R Foundation for Statistical Computing, Vienna, Austria. URL https://www.R-project.org/.

Reis, J. P. A., Figueiredo, S. A. C., Sousa, M. L., & Leão, P. N. (2020). BrtB is an O-alkylating enzyme that generates fatty acid-bartoloside esters. *Nature Communications, 11*(1), 1458. doi:10.1038/s41467-020-15302-z

Resh, M. D. (1999). Fatty acylation of proteins: new insights into membrane targeting of myristoylated and palmitoylated proteins. *Biochim Biophys Acta, 1451*(1), 1-16. doi:10.1016/s0167-4889(99)00075-0

Resh, M. D. (2016). Fatty acylation of proteins: The long and the short of it. *Prog Lipid Res, 63*, 120-131. doi:10.1016/j.plipres.2016.05.002

Rippka, R. (1988). [1] Isolation and purification of cyanobacteria. In *Meth. Enzymol.,* (Vol. 167, pp. 3-27): Academic Press.

Sakamoto, T., & Bryant, D. A. (2002). Synergistic effect of high-light and low temperature on cell growth of the Delta12 fatty acid desaturase mutant in Synechococcus sp. PCC 7002. *Photosynth Res, 72*(3), 231-242. doi:10.1023/a:1019820813257

Sanchez, L., Boulanger, E., Arnal, V., Boissery, P., Dalongeville, A., Dejean, T., . . . Mouillot, D. (2022). Ecological indicators based on quantitative eDNA metabarcoding: the case of marine reserves. *Ecol. Indic., 140*, 108966. doi:https://doi.org/10.1016/j.ecolind.2022.108966

Sato, N., & Murata, N. (1980). Temperature shift-induced responses in lipids in the blue-green alga, Anabaena variabilis: the central role of diacylmonogalactosylglycerol in thermo-adaptation. *Biochim Biophys Acta, 619*(2), 353-366. doi:10.1016/0005-2760(80)90083-1

Sharma, R., Chisti, Y., & Banerjee, U. C. (2001). Production, purification, characterization, and applications of lipases. *Biotechnol Adv, 19*(8), 627-662. doi:10.1016/s0734-9750(01)00086-6

Takatani, N., Use, K., Kato, A., Ikeda, K., Kojima, K., Aichi, M., . . . Omata, T. (2015). Essential Role of Acyl-ACP Synthetase in Acclimation of the Cyanobacterium Synechococcus elongatus Strain PCC 7942 to High-Light Conditions. *Plant Cell Physiol, 56*(8), 1608-1615. doi:10.1093/pcp/pcv086

Terrific Broth (TB) Medium. (2015). *2015*(9), pdb.rec085894. doi:10.1101/pdb.rec085894

Wältermann, M., & Steinbüchel, A. (2005). Neutral lipid bodies in prokaryotes: recent insights into structure, formation, and relationship to eukaryotic lipid depots. *J Bacteriol, 187*(11), 3607-3619. doi:10.1128/jb.187.11.3607-3619.2005

Wang, L., Chen, L., Yang, S., & Tan, X. (2020). Photosynthetic Conversion of Carbon Dioxide to Oleochemicals by Cyanobacteria: Recent Advances and Future Perspectives. *11*. doi:10.3389/fmicb.2020.00634

Yao, J., & Rock, C. O. (2017). Bacterial fatty acid metabolism in modern antibiotic discovery. *Biochim Biophys Acta Mol Cell Biol Lipids, 1862*(11), 1300-1309. doi:10.1016/j.bbalip.2016.09.014

Zhang, C.-C., Zhou, C.-Z., Burnap, R. L., & Peng, L. (2018). Carbon/Nitrogen Metabolic Balance: Lessons from Cyanobacteria. *Trends in Plant Sci., 23*(12), 1116-1130. doi:https://doi.org/10.1016/j.tplants.2018.09.008

6 - Annexes

6.1 - Annex figures

	Wild-type		*Aas* Knock-out	
Lipid family	**Non labelled Mass**	**labelled mass (+23,14)**	**Non labelled mass**	**Labelled mass (+23,14)**
PG				
PG				
PG (PC)				
PG 18:2/16:1				
PG 18:1/16:1				
SQDG 34:2				
SQDG 32:0				
SQDG 34:3				

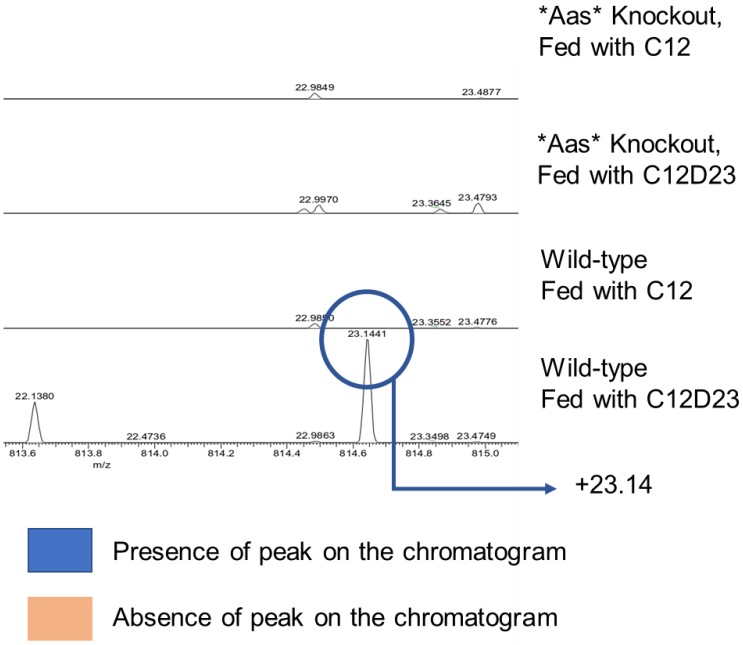

Annex Figure 1 – Feeding assay performed to detect lipid incorporation in PCC 6803 Aas KO using deuterated C12 fatty acid. Wild-type incorporation was used as a control. No lipid incorporation of labelled FAs was detected in the genetic KO of the Aas. All assays were performed in triplicate.

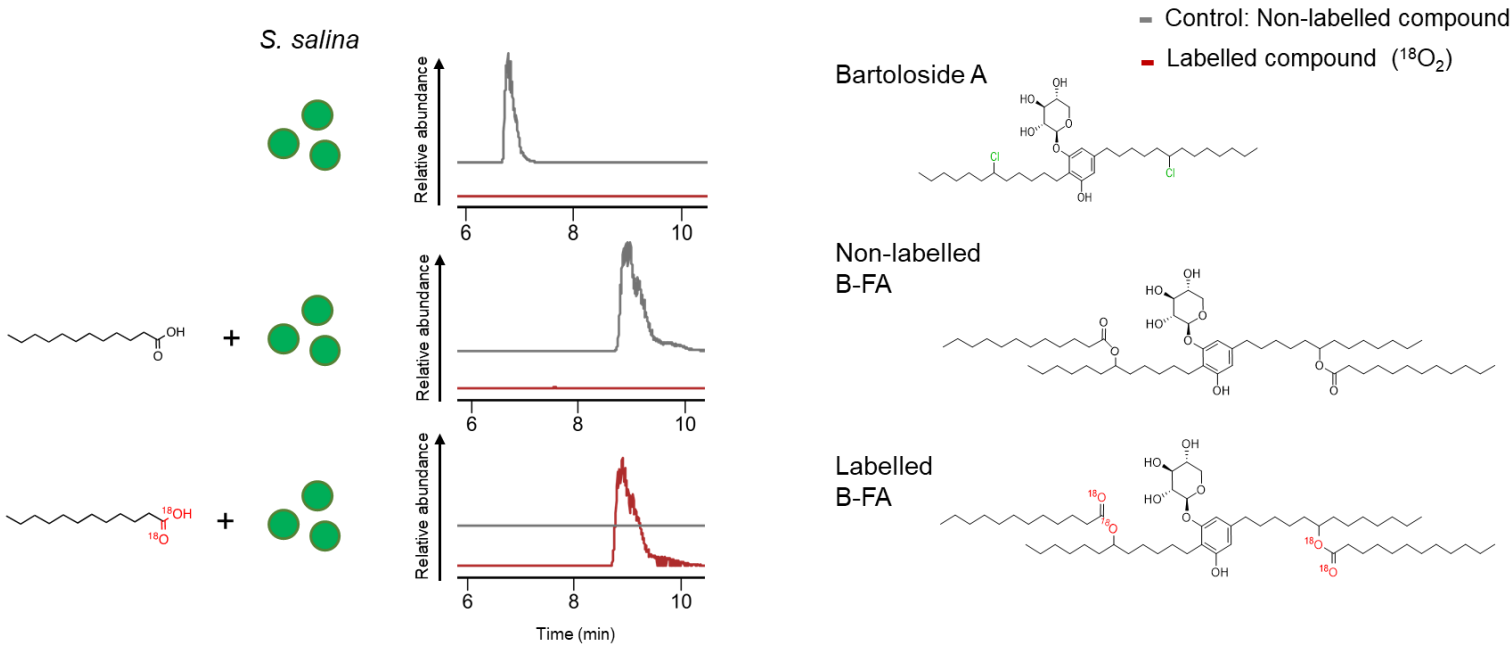

Annex Figure 2 - *S. salina* 06099 eFAs incorporation was tested using the heavy stable oxygen isotope ^{18}O. It is observed that through BrtB, both 18O are incorporated directly (without prior activation by the Aas) into B-FAs. All assays were performed in triplicate.

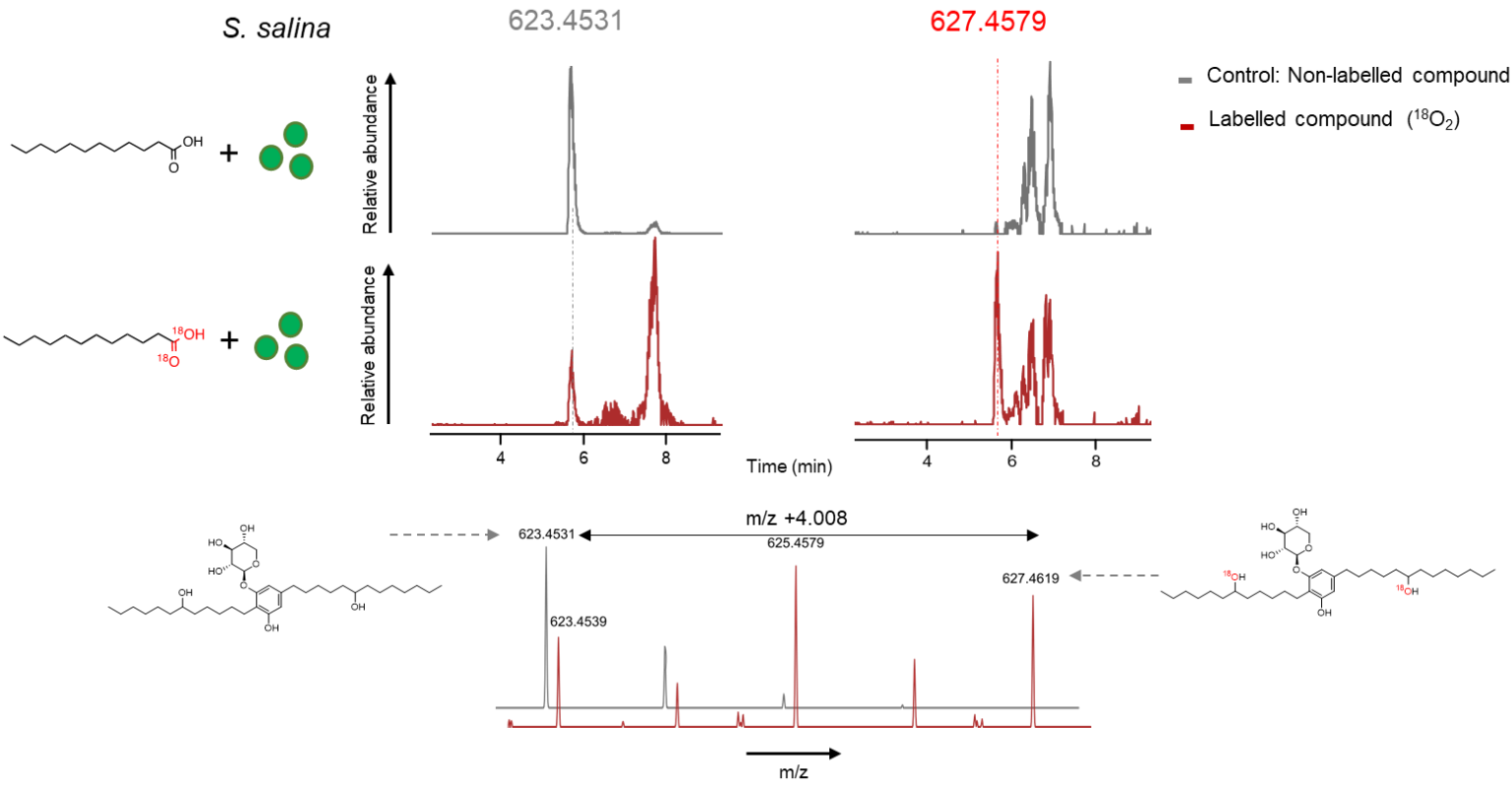

Annex Figure 3 - *S. salina* 06099 eFAs hydrolysis was tested using the heavy stable oxygen isotope ^{18}O. It was found that B-FAs which incorporated the labelled oxygen directly were hydrolyzed afterwards, by observing the bartolosides from which the labelled FAs would have been cleaved. In cultures supplemented with the oxygen isotope an increase of 4.008 is seen, which corresponds to the added mass of ^{18}O present. All assays were performed in triplicate.

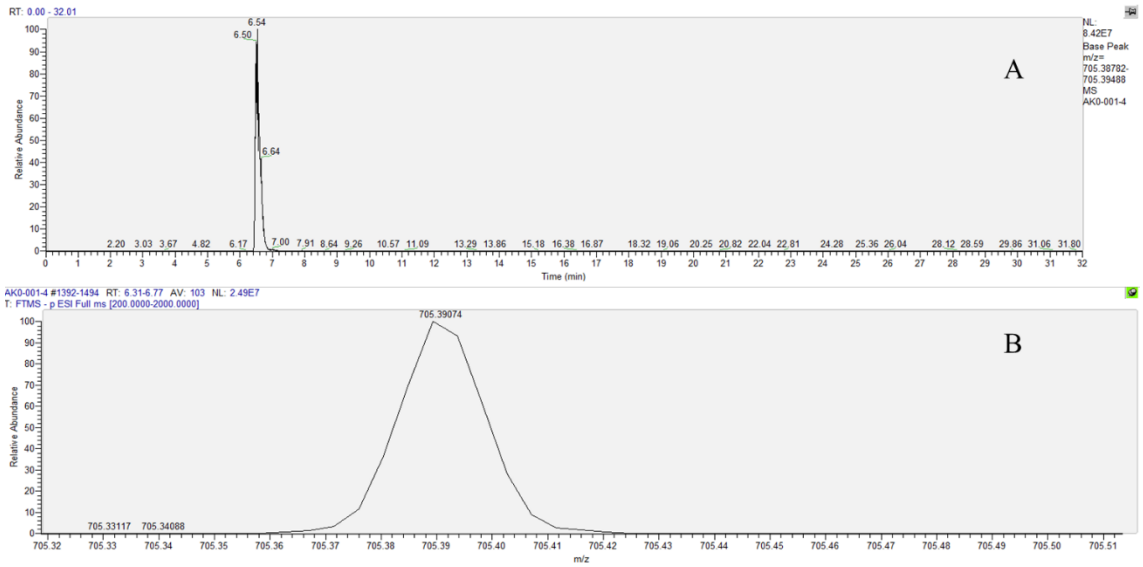

Annex Figure 4 - Example of the Xcalibur program used. Figure A displays peak for the mass corresponding to Bartoloside A, and Figure B displays the exact mass present in the observed peak. A mass tolerance of 5.0 in ppm was used with 5 decimals. This process was repeated for each B-FA mass.

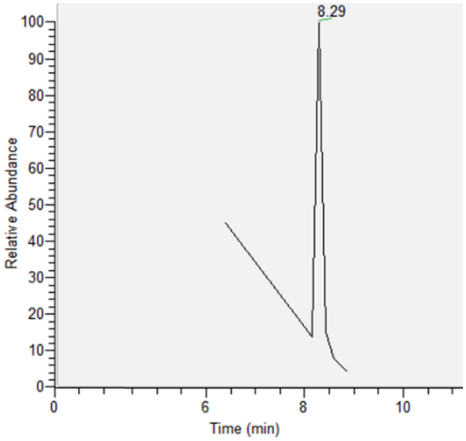

Annex Figure 5 - Example of an MS2 peak in Xcalibur. Peak represents mass equivalent to that of B-FA C16, one of the most abundant B-FAs in *S. salina* 06099.

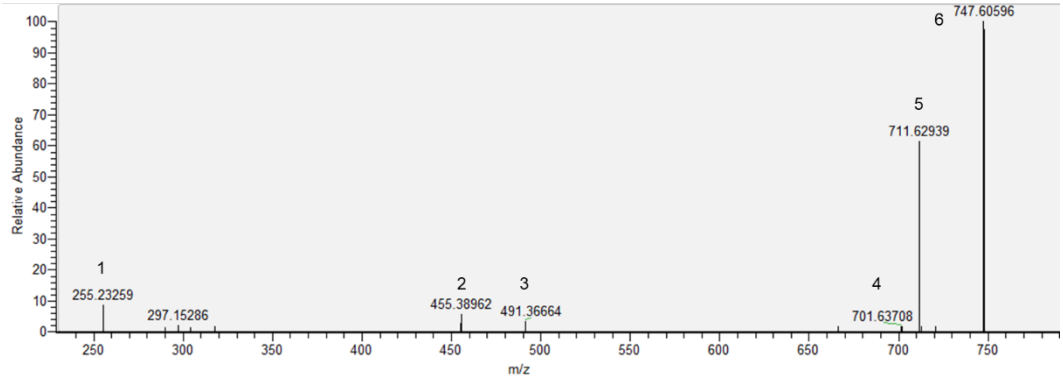

Annex Figure 6 - Follow up to figure 5, this figure shows the fragmentation of the observed mass peak. Using Reis et al. paper it is possible to confirm all of the fragments that constitute B-FA C16 in the MS2 data. This process was repeated for all masses.

6.2 - Annex tables

Annex Table 1 – Bartoloside ANOVA statistical analysis in relation to temperature and time (check figure 8) using functions lm and shapiro.test. Intercept represents day 0 at 17°C, while Temp23°C and Temp30°C represent the decreases of bartoloside in relation to the intercept. Log(Day) represents the decrease of bartoloside per time point of data. Every temperature is significantly different from each other.

Bartoloside statistical analysis in relation to temperature and time		
Coefficients:	Estimate StD	t Value Pr(>|t|)
Intercept(17°C)	149.282	22.25<0.001 ***
Temp23°C	-48.407	-13.41<0.001 ***
Temp30°C	-55.883	-16.03<0.001 ***
log(Day)	-26.83	-14.39<0.001 ***
Significance codes: 0 - '***' 0.001 - '**' 0.01 - '*' 0.05 - '.' 0.1 - ' ' 1.		

Annex Table 2 – ANOVA analysis confirming significant difference in Bartolosides between temperature and time.

Anova (Type II tests) Bartoloside analysis		
	Df	F value Pr(>F)
Temp	2	134.08 < 0.001 ***
log(Day)	1	207.06 < 0.001 ***
Residual	46	

Annex Table 3 – Multiple comparison with Tukey Test, comparing bartolosides in each of the 3 temperatures with each other. Each row compares two different temperatures. Estimate values represent difference of bartoloside between temperatures. Every pair is significantly different from each other.

Bartoloside multiple comparisons: Tukey Contrasts in relation to temperature and time		
Linear Hypothesis	Estimate StD.	t Value Pr(>|t|)
23 – 17 == 0	-48.407	-13.409<0.001 ***
30 – 17 == 0	-55.883	-16-026<0.001 ***
30 – 23 == 0	-10.476	-3.829<0.01 **
Significance codes: 0 - '***' 0.001 - '**' 0.01 - '*' 0.05 - '.' 0.1 - ' ' 1.		

Annex Table 4 - B-FA ANOVA statistical analysis in relation to temperature and time (check figure 8) using functions lm and shapiro.test. Intercept represents day 0 at 17°C, while Temp23°C and Temp30°C represent the decreases of bartoloside in relation to the intercept. Log (Day) represents the decrease of bartoloside per time point of data. Every temperature is significantly different from each other.

B-FAs statistical analysis in relation to temperature and time		
Coefficients:	Estimate StD.	t Value Pr(>|t|)
Intercept(17°C)	51.177	20.98<0.001 ***
Temp23°C	-17.608	-13.36<0.001 ***
Temp30°C	-19.908	-15.23<0.001 ***
log(Day)	-8.220	-12.23<0.001 ***
Significance codes: 0 - '***' 0.001 - '**' 0.01 - '*' 0.05 - '.' 0.1 - ' ' 1.		

Annex Table 5 - ANOVA analysis confirming significant difference in B-FAs between temperature and time.

Anova (Type II tests) B-FA analysis		
	Df	F value Pr(>F)
Temp	2	118.12 < 0.001 ***
log(Day)	1	149.63 < 0.001 ***
Residual	46	

Annex Table 6 - Multiple comparison with Tukey Test, comparing B-FAs in each of the 3 temperatures with each other. Each row compares two different temperatures. Estimate values represent difference of B-FAs between temperatures. Every pair is significantly different from each other.

B-FA multiple comparisons: Tukey Contrasts in relation to temperature and time		
Linear Hypothesis	Estimate StD.	t Value Pr(>|t|)
23 – 17 == 0	-17.6076	-13.356<0.001 ***
30 – 17 == 0	-19.9078	-15.230<0.001 ***
30 – 23 == 0	-2.3001	-2.732<0.05 *
Significance codes: 0 - '***' 0.001 - '**' 0.01 - '*' 0.05 - '.' 0.1 - ' ' 1.		

Annex Table 7 – perMANOVA analysis of B-FA diversity. Adjusted p-value represents the difference between all B-FAs globally between conditions. All results were significantly different.

PerMANOVA statistical analysis in B-FA diversity	
	Adjusted p-value
17°C fed	0.004
17°C non-fed	0.004
23°C fed	0.004
23°C non-fed	0.004
Total	0.0009

Annex Table 8 – Comparing the groups defined by temperature and condition, in the Bartolosides from CO_2 depletion condition, significant differences were found globally (Kruskal-Wallis test, chi-squared= 9.46; df=3, p= 0.024). Between samples, 23°C non-fed is significantly different from 23°C fed and 17°C fed. Kruskal-Wallis tests were used instead of Mann-Whitney tests due to the low sample size.

Kruskal-Wallis test for Bartoloside in CO_2 depletion condition			
	17°C fed	17°C non-fed	23°C fed
17°C non-fed	0.525		
23°C fed	0.987	0.324	
23°C non-fed	0.081	0.738	0.033

Annex Table 9 - Comparing the groups defined by temperature and condition, in the B-FA from CO_2 depletion condition, significant differences were found globally (Kruskal-Wallis test, chi-squared= 9.359; df=3, p= 0.02488). Kruskal-Wallis tests were used instead of Mann-Whitney tests due to the low sample size.

Kruskal-Wallis test for B-FA in CO_2 depletion condition			
	17°C fed	17°C non-fed	23°C fed
17°C non-fed	0.387		
23°C fed	0.942	0.137	
23°C non-fed	0.218	0.987	0.061

Annex Table 10 - Comparing the groups defined by temperature and condition, in the Bartolosides from CO_2 depletion and constant light condition, significant differences were found globally (Kruskal-Wallis test, chi-squared= 9.4615; df=3, p= 0.02374). Between samples, 23°C non-fed is significantly different from 23°C fed and 17°C fed. Kruskal-Wallis tests were used instead of Mann-Whitney tests due to the low sample size.

Kruskal-Wallis test for Bartoloside in CO_2 depletion and constant light condition			
	17°C fed	17°C non-fed	23°C fed
17°C non-fed	0.324		
23°C fed	0.987	0.525	
23°C non-fed	0.033	0.738	0.081

Annex Table 11 - Comparing the groups defined by temperature and condition, in the B-FA from CO_2 depletion condition, significant differences were found globally (Kruskal-Wallis test, chi-squared= 8.7436; df=3, p= 0.0329). Kruskal-Wallis tests were used instead of Mann-Whitney tests due to the low sample size.

Kruskal-Wallis test for B-FA in CO_2 depletion and constant light condition			
	17°C fed	17°C non-fed	23°C fed
17°C non-fed	0.387		
23°C fed	0.942	0.137	
23°C non-fed	0.218	0.987	0.061

Annex Table 12 – Table composed of all masses used to analyze bartoloside and B-FA production and diversity. Adduct mass represents the mass increase after samples are ionized through LC-MS. All masses were obtained using ChemDraw. Graphs were made using R.

Bartoloside A FAs				
C18:3 - bartoloside A FA	Monoester	Adduct	DiE	Adduct
	901.633	947.63928	1143.88087	1189.88715
C18:2 - bartoloside A FA	Monoester	Adduct	DiE	Adduct
	903.649	949.65528	1147.91217	1193.91845
C18:1 - bartoloside A FA	Monoester	Adduct	DiE	Adduct
	905.664	951.67028	1151.94347	1197.94975
C18- bartoloside A FA	Monoester	Adduct	DiE	Adduct
	907.68	953.68628	1155.97477	1201.98105
C16-Bartoloside A FA	Monoester	Adduct	DiE	Adduct
	879.64862	879.64862	1099.91217	1099.91217
C14-Bartoloside A FA	Monoester	Adduct	DiE	Adduct
	851.617	897.62328	1043.84957	1089.85585
C12-Bartoloside A FA	Monoester	Adduct	DiE	Adduct
	823.58602	869.59230	987.78697	1033.79325
C10-Bartoloside A FA	Monoester	Adduct	DiE	Adduct
	795.55472	841.56100	931.72437	977.73065
C8-Bartoloside A FA	Monoester	Adduct	DiE	Adduct
	767.52342	813.52970	875.66177	921.66805
C6-Bartoloside A FA	Monoester	Adduct	DiE	Adduct
	739.49212	785.49840	819.59917	865.60545
C4-Bartoloside A FA	Monoester	Adduct	DiE	Adduct
	711.46082	757.46710	763.53657	809.54285
C2-Bartoloside A FA	Monoester	Adduct	DiE	Adduct
	683.42952	729.43580	707.47397	753.48025

U.PORTO

FACULDADE DE CIÊNCIAS
UNIVERSIDADE DO PORTO

MSc

2.º
CICLO

FCUP
2022

U.PORTO

Cellular localization and eco-physiological relevance of a new enzyme and its products involved in exogenous fatty acid incorporation in cyanobacteria

Ricardo Queirós

FC

U.PORTO

FACULDADE DE CIÊNCIAS
UNIVERSIDADE DO PORTO

Cellular localization and eco - physiological relevance of a new enzyme and its products involved in exogenous fatty acid incorporation in cyanobacteria.

Ricardo Queirós

Dissertação de Mestrado apresentada à
Faculdade de Ciências da Universidade do Porto em
Biologia Funcional e Biotecnologia de Plantas

2022

MSc

2.º CICLO